JOURNAL OF ENGINEERING SCIENCES

Volume 7, Issue 1 (2020)

Huliienko S. V. Korniienko Y. M., Gatilov K. O. (2020). Modern trends in the mathematical simulation of pressure-driven membrane processes. Journal of Engineering Sciences, Vol. 7(1), pp. F1–F21, doi: 10.21272/jes.2020.7(1).f1

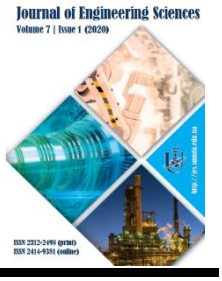

Modern Trends in the Mathematical Simulation of Pressure-Driven Membrane Processes

Huliienko S. V.[1*[0000-0002-9042-870X]], Korniienko Y. M.[1[0000-0002-3031-6212]], Gatilov K. O.[2]

[1] National Technical University of Ukraine "Igor Sikorsky Kyiv Polytechnic Institute", 37 Peremohy Ave., 03056 Kyiv, Ukraine;
[2] Archer Daniels Midland Company ADM Europoort B.V., 125, Elbeweg, 3198 LC, Rotterdam, Netherlands

Article info:
Paper received: December 6, 2019
The final version of the paper received: March 19, 2020
Paper accepted online: April 2, 2020

***Corresponding email:**
sergii.guliienko@gmail.com

Abstract. The presented article is an attempt to evaluate the progress in the development of the mathematical simulation of the pressure-driven membrane processes. It was considered more than 170 articles devoted to the simulation of reverse osmosis, nanofiltration, ultrafiltration, and microfiltration and the others published between 2000 and 2010 years. Besides the conventional approaches, which include the irreversible thermodynamics, diffusion and pore flow (and models which consider the membrane surface charge for nanofiltration process), the application of the methods the computational fluid dynamics, artificial neural networks, optimization, and economic analysis have been considered. The main trends in this field have been pointed out, and the areas of using approaches under consideration have been determined. The technological problems which have been solved using the mentioned approaches have also been considered. Although the question of the concentration polarization has not been considered separately, it was defined that, in many cases, the sufficiently accurate model cannot be designed without considering this phenomenon. The findings allow evaluating more thoroughly the development of the simulation of pressure-driven membrane processes. Moreover, the review allows choosing the strategy of the simulation of the considered processes.

Keywords: membrane, simulation, model, reverse osmosis nanofiltration, ultrafiltration, microfiltration.

1 Introduction

The pressure-driven membrane processes, including reverse osmosis (RO), nanofiltration (NF), ultrafiltration (UF), and microfiltration (MF) are widely used in the chemical industry and the related industries such as the food and pharmaceutical processing, the utilities and the environment protection [1].

The development of these processes as industrial separation technics has been started in the 1960s, and during several decades they became widespread in the mentioned above industries. It was determined by the set of advantages of the pressure-driven membrane processes, primarily by the low energy consumption and by the high effectiveness of separation, the absence of the requirement of chemicals, and the simplicity of equipment design [1].

The mathematical simulation plays an essential role in the design and investigation of these processes. It allows reducing the number of experiments and hence reducing the financial costs and energy consumption. Since the 1960s, it was proposed several ways in the simulation of pressure-driven membrane processes, but the unitary approach has not been developed.

Moreover, some attempts to review these models have been made, for example, by Soltanieh and Gill [1], Williams [2], and Sobana and Panda [3]. But in mentioned works even in relatively new [3], the primary attention is dedicated to the conventional models developed in the 1960s and 1970s, and modern approaches to the simulation of pressure-driven membrane processes are not regarded enough. Besides, these reviews have been dedicated only to reverse osmosis when the attention to the other processes has been lower.

This work is an attempt to consider more novel approaches to simulation of pressure-driven membrane processes. Due to a large number of published materials since 2000, the scope of this amount of information is quite difficult, so it was decided to make a review for the first decade of the XXI century. The review of publication for 10 years is an adequate task and provides an opportunity for carrying out of analogical reviews for further decades or lover periods.

Therefore, the main aims of the estimation of the current review are the determination of the main trends in the development of the mathematical simulation of the pressure-driven membrane processes in the chosen period and the designation of the reasonable areas for application

of different approaches to simulation. The objectives include (i) the estimation of using of the conventional mathematical models of RO, NF, and UF; (ii) the review of the novel methods of simulation which were not wholly considered in previously published works; (iii) the determination of the practical problems which are most effectively solved with using of each approach to the simulation; (iv) the estimation of the perspectives of the development in the mathematical simulation of the pressure-driven membrane process.

For these purposes, more than 170 articles that have been published in the leading topical journals, primarily in "Journal of Membrane Science" and "Desalination" from 2000 to 2010, have been chosen for review. The distribution by the years represented in Fig. 1 shows that interest to the considered subject is maintained on almost the same level with the low trend to increase in later years.

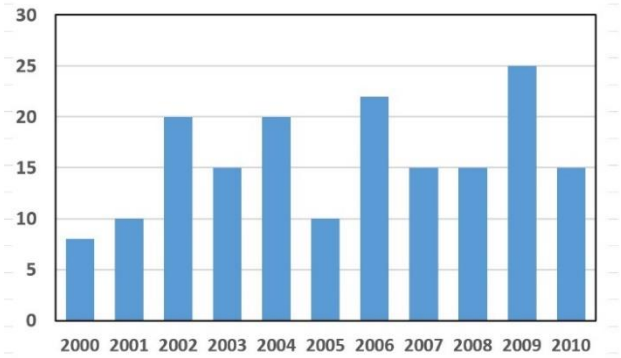

Figure 1 – The distribution of the chosen publications by years

The review does not claim to comprehensiveness, but it allows monitoring the main trends in the pressure-driven membrane process simulations in the chosen period with sufficient coverage.

2 General approaches

The publications, chosen for analysis, are dedicated to the simulation of main pressure-driven membrane processes such as RO, NF, UF, and MF and some other processes, including the preparation of membranes. The distribution of publications among the processes is shown in Fig.2, considering that some particular articles have been devoted to the simulation of several processes. It should be noticed that researches dedicated to simulations of pressure-driven membrane processes in general (for example, based on irreversible thermodynamic or computational fluid dynamics), for convenience have been attributed to RO.

In works [1–3], the conventional classification of models of pressure-driven membrane processes (primarily reverse osmosis) has been represented. It includes the models based on the irreversible thermodynamics (the membrane is considered as a "black box"), the models based on the diffusion (the active layer of membrane is considered as homogenous), and models based on the pore flow (the active layer is assumed to be micro- or macroporous). Also, in work [2], the models which consider the membrane surface membrane charge have been considered for the simulation of the NF process. However, the use of computational fluid dynamics (CFD) and artificial neural networks (ANN) Have not been considered. It should be noticed that two last approaches began to develop in the 1990s due to progress in computer technologies and the appearance of specialized software. Moreover, the topic of process control and optimization has been represented only by Sobana and Panda [3], and economic topics have been considered only by Soltanieh and Gill [1].

In the current review, the simulation of each pressure-driven membrane process has been considered separately, and within each section, the ways of simulation of process under consideration have been analyzed.

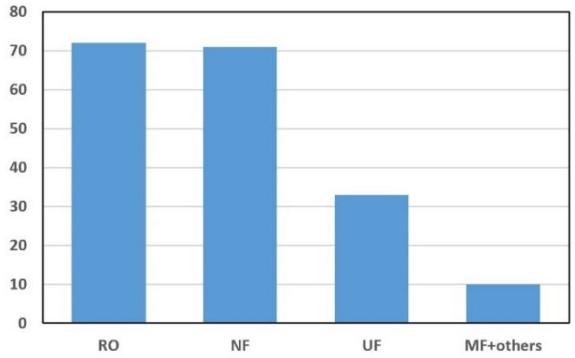

Figure 2 – The representation of models of pressure-driven membrane processes in chosen articles

The topics of concentration polarization and membrane fouling have been considered only in a case when they were a supplement of the membrane separation model. These phenomena themselves are reasonable for a particular review.

3 Reverse osmosis

3.1 Classification of reverse osmosis models

The models of the RO process, in general, can be classified in the same way as the pressure-driven membrane processes as a whole. The distribution of the models in the chosen publications by corresponding classes is shown in Fig. 3.

It should be noticed that significant numbers of models are based on irreversible thermodynamics and computational fluid dynamics. Also, many papers are dedicated to problems of process control and optimization. On the other hand, the pore flow-based models are considered in a much smaller number of works, if the CFD approach would not consider.

3.2 Irreversible thermodynamics models

It was mentioned by Williams [2], that irreversible thermodynamics models were one of the earlies RO models, and they considered membrane as a "black box". In particular, the Kedem–Katchalsky model is one of them.

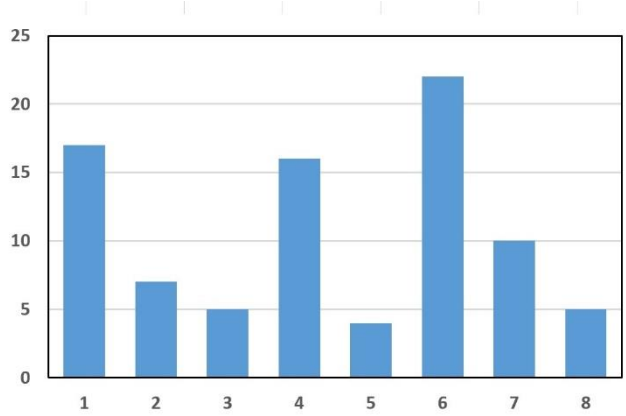

Figure 2 – The number of RO models in chosen articles by classes: 1 – irreversible thermodynamics based models; 2 – diffusion-based models; 3 – pore flow-based models; 4 – CFD based models; 5 – ANN-based models; 6 – process control and optimization; 7 – economic analyses; 8 – other models

This model assumes that the membrane is in conditions close to equilibrium [2], and the solvent (water) flux can be described by the phenomenological equation in a form [4]:

$$J_w = L_p \Delta p - L_p \sigma \Delta \pi \tag{1}$$

where Δp is the applied pressure; $\Delta\pi$ is the osmotic pressure difference; L_p and σ are the phenomenological constants.

The solute (salt) flux, according to this model, can be described by equation [4]:

$$J_s = \omega \Delta \pi + (1-\sigma) c_m J_w \tag{2}$$

where c_m is the average solute concentration in the membrane; ω is the phenomenological constant.

The determination of phenomenological constants is the main problem in using ~~of~~ this model. Moreover, this constant are functions of concentration [2, 3]. Some analytical research with this model, including the studies with the aim to determine relationships for calculation of these parameters, were carried out by Jarzynska M. [4], Koter [5], and Kargol [6, 7].

For estimation of RO selectivity in this model, the value of the rejection rate of solute is used [3]:

$$R = 1 - \frac{c_p}{c_f} \tag{3}$$

where c_p is the permeate concentration; c_f is the feed concentration.

The expression for the calculation of this value can be obtained using equation (1) and equation (2) [2]:

$$\frac{1}{R} = \frac{1}{\sigma} + \left(\frac{L_\pi}{L_p} - \sigma^2 \right) \left(\frac{L_p}{\sigma} \right) \pi_f \frac{1}{J_w} \tag{4}$$

The phenomenological constant ω in equation (4) is expressed by relationship [2]:

$$\omega = \left(\frac{L_\pi}{L_p} \right) c_m L_p \tag{5}$$

The Kedem-Katchalsky model in years under consideration was used for simulation of the hydrated particles transport through the membrane [8], the development of the system approach to simulations of mass transfer through the membrane considering both convection and diffusion [9], the optimization of the seawater desalination in the tubular membrane [10], and for considering the influence of boundary layers on RO process [6]. However, the application of this model was limited, which is in agreement with Williams' conclusion [2].

The Spiegler–Kedem model was the most crucial development of the Kedem–Katchalsky model. According to this approach, the solvent and solute fluxes are described by equations [11]:

$$J_w = -p_h \left(\frac{dp}{dx} - \sigma \frac{d\pi}{dx} \right) \tag{6}$$

$$J_s = -p_s \frac{dC}{dx} + (1-\sigma) J_w c_m \tag{7}$$

where p_h is the specific hydraulic permeability coefficient; p_s is the local solute permeability coefficient. The application of these coefficients, according to Hyung and Kim [11] allows avoiding the dependence of the phenomenological constant values from concentrations. The rejection rate, in this case, can be obtained from equation (6) and (7) in a form [11]:

$$\frac{R}{1-R} = \frac{\sigma}{1-\sigma} \cdot \frac{1 - \exp\left(-J_w \cdot (1-\sigma)/P_s\right)}{\exp\left(-J_w / k\right)} \tag{8}$$

where P_s is the overall permeability constant; k is the mass transfer coefficient. The P_s value can be defined as follows [11]:

$$P_s = p_s / \Delta x \tag{9}$$

where Δx is the membrane skin layer thickness.

The mass transfer coefficient values are defined from the objective laws of mass transport in membrane modules, usually from dimensionless equations [1].

The advantages of the Spiegler–Kedem model caused its more comprehensive application than the Kedem-Katchalsky model. In the first decade of the XXI century, the modifications of this model were designed for different kinds of membrane modules, including spiral-wound [12], tubular [13], and hollow-fiber [14, 15]. The modifications are also carried out for the cases of separation of specific solutions, for example, boron removal [11, 16], separations of sodium sulfate and sodium chloride [17], ammonium fumarate [18], brackish water desalination [9] and wastewater treatments from palm oil productions [19]. The application of the Spiegler-Kedem model was

especially useful in conjunction with the models of concentration polarization.

Despite that, the irreversible thermodynamics models do not consider the membrane structure [2], in they involve the relatively simple equations for the RO process describing. Also, sophisticated solving methods are not necessary. These reasons determined the quite extensive usage of mentioned models in the early XXI century.

3.3 Diffusion based models

The models of this class are based on the assumption that the membrane skin layer is non-porous. Therefore, the mass transfer is governed by diffusion [21]. In this case, Fick's law is the basis of the mathematical description of processes [22]:

$$J_i = -D_i \frac{dC_i}{dx} \tag{10}$$

where J_i is the flux of *i*-component through the membrane; D_i is the diffusivity coefficient of *i*-component; C_i is the concentration of *i*-component; *x* is the direction of mass flux through the membrane.

The solution-diffusion model has been the most widely used in this class. The primary assumption of it is following [1, 2, 21, 22]: (i) membrane includes a homogenous non-porous skin layer; (ii) both solute and solvent can dissolve in the membrane material, and both of them can diffuse through the membrane; (iii) the diffusion of solute and solvent is independent of each other since each of components is passed due to its gradient of chemical potential; (iv) the gradients of chemical potential are determined by pressure and concentration difference across the membrane. In this case, the separation of solution would be occurring due to the difference in diffusion rates of components.

By the integration and transformations of the equation (10), the solvent flux can be represented in a form [21]:

$$J_w = \frac{D_w \cdot C_w \cdot V_w}{R \cdot T \cdot \delta}\left(\Delta p - \Delta\pi\right) \tag{11}$$

where D_w is the diffusivity coefficient of the solvent (water) in membrane material; C_w is the solvent concentration in membrane material; V_w is the partial molar volume of solvent; *R* is the ideal gas constant; *T* is the absolute temperature; δ is the membrane thickness.

To simplify the equation (11), it can be suggested the designation in a form [21]:

$$A = \frac{D_w \cdot C_w \cdot V_w}{R \cdot T \cdot \delta} \tag{12}$$

Then the equation (11) can be rewritten [21]:

$$J_w = A\left(\Delta p - \Delta\pi\right) \tag{13}$$

For the case of solute, the integration of equation (10) gives the result [22]:

$$J_s = \frac{D_s \cdot K_s}{\delta}\left(C_f - C_p\right) = B \cdot \left(C_f - C_p\right) \tag{14}$$

where D_s is the solute diffusivity coefficient in membrane material; K_s is the partition coefficient; C_f is the solute concentration in feed solution; C_p is the solute concentration in permeate.

Correspondingly, the rejection rate defined by the simultaneous solution of equation (13) and equation (14) can be represented in a form [2]:

$$\frac{1}{R} = 1 + \left(\frac{B}{A}\right)\left(\frac{1}{\Delta p - \Delta\pi}\right) \tag{15}$$

The quite extensive use of the solution-diffusion model, as I a case of irreversible thermodynamics models, is linked with its simplicity [22]. In the period under consideration, this model was applied to the description of the RO process for both water solutions [23-25] and organic systems [21, 22]. Also, it has been used for the development of hybrid models [26] and the theoretical analysis of the mass transfer through the membrane [27]. Furthermore, the modifications of the solution-diffusion model were proposed. They consider the concentration polarization [24], the sorption equilibrium between membrane material and organic matter [22], and nonlinear relationships among the mass transfer coefficient and the operation parameters of the process [26, 27].

Except discussed above solution-diffusion model, among solution based RO models Soltanieh and Gill [1] and Williams [2] also emphasized the solution-diffusion-imperfection model and the extended solution-diffusion model. These models were absent in the publication chosen for review, so for completeness, the characteristics of these models are considered based on the earlier reviews.

The solution-diffusion-imperfection model considers the pore flow as an addiction to the diffusion of components of the solution as a transport mechanism. This accepts that the small imperfections or defects (pores) can exist on the membrane surface, through which the mass transport can take place [1, 2]. In this case, the solvent and solute flaxes can be described by equations in a form [1, 2]:

$$N_w = K_1 \cdot \left(\Delta p - \Delta\pi\right) + K_2 \cdot \Delta p = J_w + K_2 \cdot \Delta p \tag{16}$$

$$N_s = K_3\left(c_f - c_p\right) + K_2 \cdot \Delta p = J_s + K_2 \cdot \Delta p \tag{17}$$

where K_1 is the water permeability coefficient; K_2 is the coupling coefficient, which describes pore flow; K_3 is the solute permeability coefficient.

According to this model, the rejection rate can be expressed in a form [1, 2]:

$$\frac{1}{R} = 1 + \left(\frac{K_3}{K_1}\right)\left(\frac{1}{\Delta p - \Delta\pi}\right) + \left(\frac{K_2}{K_1}\right)\left(\frac{\Delta p}{\Delta p - \Delta\pi}\right) \tag{18}$$

According to Williams [2], despite that the solution-diffusion-imperfection model shows good agreement with experimental data, it has two key disadvantages. It includes three parameters, so it is necessary to use the nonlinear regression for defining the system

characteristics. Moreover, the parameters which describe the membrane system usually are the functions of concentrations and pressure.

The extended-solution-diffusion model was proposed for describing of organic solutions separation by reverse osmosis. In this case, it is necessary to consider the influence of pressure on the chemical potential of the solvent, which does not consider in the solution-diffusion model [2]. Then the solute flux can be represented in a form [2]:

$$J_s = \frac{D_{sm} \cdot K_{sm}}{\delta}\left(c_f - c_p\right) + L_{sp} \cdot \Delta p \tag{19}$$

where L_{sp} is the parameter that is responsible for the solute transport due to pressure difference across the membrane.

The rejection rate is determined from equation [2]:

$$\frac{1}{R}\left[1 - \frac{L_{sp}}{A \cdot C_F}\left(1 - \frac{\Delta\pi}{\Delta p}\right)\right] = 1 + \frac{B}{A \cdot \left(\Delta p - \Delta\pi\right)} \tag{20}$$

Despite that this model can adequately describe the separation of phenols by cellulose acetate membranes, it did not find the full application [2].

The general disadvantage of discussed in this section models is the overestimation of the water flux values during the separation of the dilute organic solutions.

3.4 Pore flow-based models

Unlike the diffusion-based models, the models of this class consider the skin layer as microporous. In this case, the mass transfer occurs by both diffusion and convection [1, 2].

The preferential sorption-capillary flow model is the most widely used in this class [1, 2, 28]. It is also known as the Kimura–Sourirajan model [23, 30]. According to it, the skin layer has specific chemical properties such as the preferential sorption of solvent and preferential repulsion of solutes. As a result, on the membrane surface and inside the pores, the layer of almost pure solvent is formed. The transport of solutions is occurred due to passing the solvent molecules from this layer through the pores under applied pressure [1, 2].

According to the model under consideration, the solvent flux can be expressed in a form [1, 2, 28–30]:

$$N_w = A\left(\Delta p - \left(\pi\left(x_f\right) - \pi\left(x_p\right)\right)\right) \tag{21}$$

where A ~~the~~ is pure solvent permeability constant. The values of osmotic pressures in feed solution and permeate in this case are represented as functions of concentrations, which usually expressed in molar fractions [1].

The solute flux can be described by the equation [1, 2, 28–30]:

$$N_s = \frac{D_{sp} K_D c}{\delta}\left(x_f - x_p\right) \tag{22}$$

where K_D is the distribution coefficient of solute in membrane pores.

In this case, the rejection rate cam defined from relationship [1, 2, 28–30]:

$$\frac{1}{R} = 1 + \frac{D_{sp} K_D C_t}{\delta} \cdot \frac{1}{A\left(\Delta p - \left(\pi\left(x_f\right) - \pi\left(x_p\right)\right)\right)} \tag{23}$$

In the period under consideration, the preferential sorption-capillary flow model was used for the analysis of organic components (benzene and toluene) with modification to consider the membrane-solute interaction [28] and determinations of the objective laws of mass transfer in such systems [30], and also for the case of seawater desalination with regarding of concentration polarization [29]. In should be noticed that Kumano and al. [28] used the cylindrical coordinate system for the process analysis in hollow-fiber modules.

The surface force-pore flow model is another model of this class. According to it, the differential equation for velocity profiles inside the pore $\alpha(\rho)$ can be obtained by balancing the applied forces in the axial direction of the pore (z-axis). This equation considers the net force resulting from the pressure difference, the viscous stress with the application of Newtonian law of viscosity, and net force determined by frictions between solute and pore walls. As a result, this equation can be written in the form [17]:

$$\frac{d\alpha}{d\rho} + \frac{1}{\rho}\frac{d\alpha}{d\rho} + \frac{\Delta P - \Delta\Pi\left(1 - e^{-\Phi(\rho)}\right)}{\beta_1} - \frac{\alpha(\rho) e^{-\Phi(\rho)}}{\beta}\left(1 - \frac{1}{b(\rho)}\right)\left[1 + \frac{\Delta\Pi}{e^{\alpha(\rho)} - 1}\right] \tag{24}$$

The parameters β1, ΔP, ΔΠ, b, Φ, and ρ according to Jain and Gupta [17] are expressed through the properties of the solution (viscosity, diffusivity coefficient an osmotic pressure), the operation parameters of the process (applied pressure), and the membrane properties (skin layer thickness, pore radius). Initial and boundary conditions must supplement the equation (24). The solution of this mathematical model is related to the application of known methods of differential equation solution. The obtained velocity profile allows defining the solute and solvent fluxes in a single pore [17]:

$$J_s = \frac{2}{X_{SW}}\frac{1}{\tau}\int_0^{1-\lambda} \frac{\alpha(\rho)}{b(\rho)}\left(\pi_2 - \frac{\pi_2 - \pi_3}{\exp(\alpha(\rho)) - 1}\right) e^{-\Phi(\rho)} d\rho \tag{25}$$

$$J_w = \frac{2}{X_{SW}}\frac{1}{\tau} C \cdot R \cdot T \int_0^1 \alpha(\rho)\rho d\rho \tag{26}$$

where X_{AB} is the ratio of the product of a gas constant and solution temperature to solute diffusivity in solution; C is the molar concentration of the solution.

The overall fluxes through the membrane are conjunct with fluxes in a single pore by the value of membrane porosity [17].

The solute concentration in permeate cam be calculated using the relationship [17]:

$$c_p = c_f \frac{J_s}{J_s + J_w} \quad (27)$$

The surface force-pore flow model is a development of the finely-porous model. The finely-porous model porous model considers the changes in parameters only in the axial direction (arose skin layer) when the surface force-pore flow model considers the changes of parameters in both axial and radial directions [2].

Since in articles, the chosen for review the finely-porous model is not represented, the general information about this model is given according to the data in earlier reviews [1, 2]. In conditions of assumptions of this approach, the overall volumetric flux can be described by Poiseuille law [1], so:

$$\varepsilon \cdot u = -\frac{\varepsilon r_p^2}{8\mu} \frac{dp}{dz} \quad (28)$$

where u is the local center of mass velocity of the fluid in pores; ε is the fractional open area; μ is the viscosity of the fluid in pores.

As in the previous model, the equation (28) must be supplemented by initial and boundary conditions, and its solution allows defining the value of the fluid velocity in the pore, which is the basis for defining the solute flux and the rejection rate.

The hypothesis about the pore structure of the membrane skin layer also has been used during the analysis of mass transfer in the membrane channel under turbulent conditions [31].

Despite that, the pore models in many cases show a good agreement with experimental results and give a clear understanding of the processes in the porous membrane skin layer, in the period under consideration they have been mentioned in the limited number of publications. The probable of this is that most models involve the derivation of differential equations systems. In the XXI century, it is advisable to use computers for derivations of such problems. For such requirements, the set of program products has been developed. In many cases, they include the methods of computational fluid dynamics (CDF). The applications of this approach are described in the next section.

3.5 Computational fluid dynamics based models

In the analysis of process during reverse osmosis, it is necessary to consider the hydrodynamic conditions, which influence directly on both separations processes (e.g. including the mass transfer intensity and the impact of concentration polarization) and the energy consumption on the transportation of feed solution.

The fluid flow is described mathematically by the Navier-Stokes equation coupled with the continuity equation, which can be written in short form as follows [32]:

$$\frac{\partial u}{\partial t} + u \cdot \nabla u = -\nabla p + \frac{1}{\mathrm{Re}} \nabla^2 u \quad (29)$$

$$\nabla \cdot u = 0 \quad (30)$$

where u is the velocity of the fluid flow; p is the pressure of the fluid; Re is the Reynolds number.

In case of consideration of mass transfer, it is necessary to consider the mass conversation equations which can be written in a form [33]:

$$\frac{\partial \rho}{\partial t} + \mathrm{div}(\rho \cdot u) = 0 \quad (31)$$

where ρ –is the density (mass concentration) of solute.

The differential equations (29)–(31) supplemented with boundary conditions allow defining the functions which describe the velocity and concentration fields in the channels of membrane modules. However, the analytical solution is possible only for the narrow range of relatively simple problems because of the complexity of the mentioned equations. Therefore, for practical purposes, the numerical methods which allow defining the values of mentioned parameters in nodal points have to be used. Such methods are called the computational fluid dynamics (CFD), which is currently are a useful tool for the considered problem solving [33]. At present, the CFD algorithms are realized by using computers, including special developed commercial available software. The relative novelty of this method should be considered in more detail.

The most used for RO simulation software include FLUENT [32, 34–39] and ANSYS, notably the CFX algorithm [40–45]. Furthermore, for this kind of modeling, the supercomputers [46] and other algorithms [47] have been used.

One of the main applications of CFD methods in the analysis of membrane processes performance, in particular RO, is the determination of the influence of spacer on the operation parameters, including flow regimes, pressure drops and intensity of concentration polarization. The main parameters of the spacer which were under investigation in considered researches are dimensions and form of the filaments and the method of its position in the membrane channel.

Indeed, Ahmad and Lau [34] investigated the influence of the cross-section shape of the filament and defined that the cylindrical shape provides the concentration factor than in the case of rectangular shape. This means that the cylindrical shape is a more rational one. Shakaib and al. [38] and Schwinge and al. [44] studied the impact of the cylindrical filament on the hydrodynamic resistance, and it was defined that the filament thickness has more significant influence in comparison with the distance between filaments. In particular, it was shown by Shakaib and al. [38] that increasing the diameter of filament in 1.5 times leads to increasing of the pressure drop in the membrane channel 3 times.

The filament disposal has estimated the influence of spacer position in membrane channels by channel width and by the angles, which characterized the spacer position relatively to mean flow direction (Fig. 4).

It was defined by Shakaib and al. [38] and Ma and Song [46] that the zigzag shape in the most rational way of

spacer filament position by the channel width since in that case the highest intensity of mass transfer is provided.

Several approaches were used for estimation of the impact of spacer position relatively to flow direction. In most cases, for this purpose, the characteristic angles are used (Fig. 4): the angle between the spacer filaments φ; the attack angle χ; and the cell slope angle ψ (since in various authors the designation of this angles is different, even the same symbol can be used for the same angle, in present work the particular designation is used). It should be noticed that the results of different authors about the optimal values of these parameters are varied. For most commercial available membrane modules φ = 90° [41], so in some researches, only this value was considered. For example, it was pointed out by Fimbres-Weihs and Wiley [41] that for the case of χ = 45°, the better results were obtained in comparison with the case of χ = 90°. However, Shakaib and al. [38] reported that the best effect was achieved when χ = 60°. Lau and al. [36] and Li and al. [42] studied the influence of angle φ, and in the first case, the optimal results were obtained in form φ = 120° and ψ = 30° [36], and in the second case optimal values were φ = 130° and χ = 30° [42]. The possible reason for this discrepancy is that in each research, the discrete set of considered angles values.

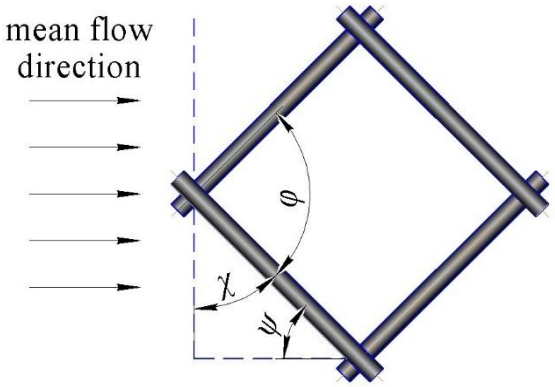

Figure 4 – The geometrical characteristic which describes the position relatively to flow direction

The other important advantage of CFD methods is flow visualization, which allows defining the critical parameters of the flow in channels with spacers. An experimental determination of these values is overstructured. In particular, in many works the critical values of the Reynolds number were determined and for different configuration of spacer the different results were obtained, including Rekr = 60 [32], Rekr = 200 and Rekr = 300 [34], Rekr = 75 and Rekr = 200 [38], Rekr = 75 and Rekr = 200 [44]. These discrepancies give evidence of the more complex character on hydrodynamical conditions in membrane channels in comparison with hollow channels.

The clear understanding of the hydrodynamical conditions the membrane channels allows clarifying the relationships for the evaluations of mass transfer intensity [35, 41] and concentration polarization [40, 45]. Moreover, Ranade and Kumar [39] carried out the comparison of the linear and nonlinear (spiral) configuration of the channels, and it was defined that the difference is negligible. Such results show that the analysis of the processes in spiral wound membrane modules with the assumption about its notional unrolling in a plate is justified.

The researches dedicated to using CFD-simulation for the analysis of the membrane process were reviewed by Ghidossi and al. [33].

3.6 Artificial neural networks based models

Except for CFD methods, using artificial neural networks (ANN) is the relatively new approach for simulations of membrane processes that had been used previously for analysis of economic systems [48, 49].

As was pointed out by Zhao and al. [26], ANN can predict any continuous relationships between input and target information. Similar to linear and nonlinear regressions, ANN develops a transforming element that allows predicting the values of the target variable for the given set of values of input variables. The physical and chemical relationships could or could not be considered directly it the neural network. Furthermore, the ANN can be applied for the phenomenological analysis of the measured data without the necessity mass transfer mechanism consideration [48] and unlike the deterministic models with are based on the physical phenomena, in ANN the additive model is used which allows relatively simple solving of the models of the complex systems without an assumption about ideal conditions [49].

In the period under consideration, the ANN has been applied for the analysis of RO water desalination effectivity [49, 50] and the economic analysis [48]. Moreover, Zhao and al. [26] carried out the comparison of the predictions of ANN with ones of the solution-diffusion model and pointed out that ANN predicts the permeate concentration more accurately. However, for the RO analysis, the application of ANN was limited.

3.7 Process control and optimization

The critical application of RO simulations is an automated process control and optimization. In this case, the mathematical models can be used for conventional [13, 51, 52] as well as for intellectual [53] control systems.

The optimization problem consists of the determination of the most advantageous values of operating parameters for process performance. During the formulation of this problem, the foremost step is the determination of the optimal criterion. In RO optimization for this purpose, the different parameters were accepted including the minimal energy consumption [25, 54, 55], the minimal cost of treated water [55-61], the maximal permeate productivity [49], the maximal rejection rate [10], and the minimal water losses during the cleaning [62]. The algorithms which were applied for the determination of the optimum values include the Levenberg–Marquardt method [19], the Newton-Gauss method [19], the response curves methods [63], the gradient methods [64], and also ANN [49].

It should be noticed that for process control and optimization, both approaches can be applied with include the models based on physical phenomena [10, 25, 51, 62, 65] and the regression models. Moreover, for this purpose, it is possible to use the simple linear and quadratic regressions [66] as well as the more accurate methods of the design of experiments and the factorial experiment [64, 67].

3.8 Economic analysis

It should be particularly noted that the methods of mathematical modeling of RO allow also carrying out the economic evaluation of the process. First of all, it refers to the seawater desalination process [56, 60]. Moreover, during the RO optimization in most cases, the choice of optimum was carried out with regarding economic parameters [54–57, 60–61], in particular the clean water price and energy consumption. The estimation of economic parameters of the process also was carried out without the optimization procedure [68], including the application of econophysics and econometrics [48], thermo-economic analysis [69], and stochastic modeling [70].

3.9 Other approaches to simulation of reverse osmosis

In particular cases, the other approaches for RO simulation can be used, including the semi-empirical model [71] and scale-up models [72]. There are some particular cases when these methods are reasonable, especially during consideration of nonconventional systems, for example, in case of using renewable energy sources (the energy of the ocean waves to generate the applied pressure) [73]. Also, the nonconventional approaches were used for the analysis of concentration polarization [74] and membrane regeneration [75], but this question should be considered apart.

4 Nanofiltration

4.1 Classification of nanofiltration models

Since the NF process is the most similar to RO, the classification of the mathematical models of this process is analogical to the described above the general classification. However, it was pointed out by Williams [2] that the characteristic feature of the NF membrane is the presence of the surface charge. Therefore, this fact allows considering the specific models based on the Donnan theory, the extended Nernst-Plank equation, and the Maxwell-Stephan equations were developed. Also, the CFD, ANN, and optimization approaches were used for simulation of the NF process. The distribution of the chosen articles by classes is shown in Fig. 5.

4.2 Irreversible thermodynamics models

As in a case of RO, the Kedem-Katchalsky and Spiegler-Kedem models are applied for the simulation of NF process; moreover, as it was shown by Ahmad [76], this approaches can be used for both cases namely the transport of the neutral components through uncharged membranes and the transport of the ions through the membrane with fixed surface charge.

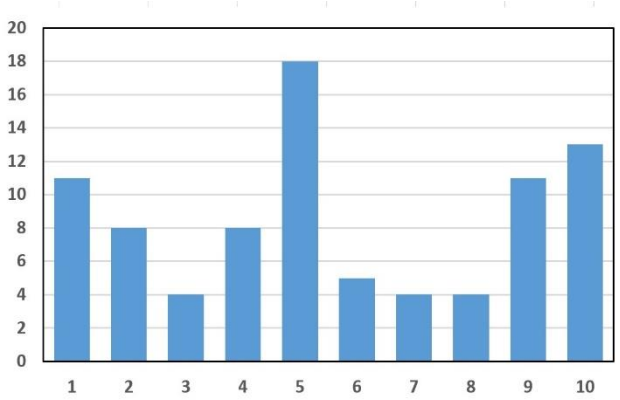

Figure 5 – The number of NF models in the chosen articles by classes: 1 – irreversible thermodynamics models; 2 – diffusion-based models, 3 – pore models; 4 – Donnan equilibrium models; 5 – extended Nernst-Plank equations based models; 6 – Maxwell-Stephan equations based models; 7 – CFD models; 8 – ANN models; 9 –optimization and economic analysis; 10 – other models

Furthermore, for describing NF, the same equations as for RO can be used. In particular, according to the Kedem-Katchalsky model the equation (1), equation (2), and equation (4) are applied, and according to the Spiegler-Kedem – the equation (6) and equation (8).

In the period under consideration, the Kedem-Katchalsky model was used for describing the periodic NF process [77] and amino acids separation [78]. At the same time, the Spiegler-Kedem model found a more comprehensive range of application, which includes the separation of the salt [79, 80] and organic components solutions [81], metabolism products of the microorganisms [18] multicomponent solutions [81], and brackish water desalination [9]. Also, this model appeared to be useful for the determinations of the characteristics of new membranes [82, 83].

In the set of researches, it was carried out the comparison of the results of the simulation using the irreversible thermodynamics with results obtained with other models, including the extender Nernst-Plank [76, 77, 81–83], solution-diffusion model [83] and artificial neural networks [79]. In that cases, it was pointed out that the Kedem-Katchalsky and Spiegler-Kedem models are more simple and required less of information [81], and the comparison with the experimental data shows that difference is 8–13 % [18, 79].

However, in some cases, when the relationships between the coefficients in the mentioned above, equations with concentration are not clearly expressed, during the simulation, the adjustment factors had to be used [20].

4.3 Diffusion based models

Despite that, the NF membranes have a skin layer with a porous structure; the diffusion-based models described in section 3.3 has also been used in some researches for the NF process analysis. As in the case of irreversible thermodynamics, the equations for RO and NF are the same, namely equation (11)–(15) for the solution-diffusion model and equation (16)–(18) for the solution-diffusion-imperfection model.

In the considered period, the solution-diffusion model was used mainly for the system containing the organic components, including polar (methanol, ethanol, isopropanol) and nonpolar (pentane, hexane, octane) solvents [21] and mixtures of alkanes, alcohols, and ketones [84]. The other applications include influent treatment, in particular X-rays indicators [85] and tannery [86] and water treatment [26]. Also, this model was useful for the determination of membrane structure and its characteristics [83] and optimization [87].

The solution-diffusion-imperfection model was also used for the description of the NF separation of organic compounds (alcohols) [88].

The comparison of the solution-diffusion model with other models, in particular the Spiegler–Kedem model [83], extended the Nernst-Plank equation [83], Maxwell-Stephan equations [84] and artificial neural networks [26], shows that other models are more suitable for the NF process description. For example, Zhao and al. [26] pointed out that the predictions of permeate concentration with the solution-diffusion model are inaccurate, and Dijkstra and al. [84] emphasized that the Maxwell-Stephan equations are a more realistic description of the process. Likely, it was a reason for the narrow range of the applications of this approach. However, in some cases, a good agreement with experimental data (difference in the range of 10–15 %) was observed [86]. The higher accuracy of the diffusion-based models can be archived by considering the concentration polarization [85, 86].

4.4 Pore flow-based models

As in a case of reverse osmosis, for the NF process simulation, the models described in section 3.4 were used in a limited range. In most cases, the transport of organic compounds, which is less influenced by the surface charge of the NF membranes. For example, Verliefde and al. [89] modified the solution for the description of the separation of the pesticides and pharmaceutical pharmaceuticals and Mattaraj, and al. [90] did the same for multicomponent mixtures containing the natural organic compounds. It should be noticed that Mattaraj and al. [90] considered the irreversible fouling formation; therefore, the stage of filtration through the cake layer was introduced into the model. The separation of ions was considered by Chaabane and al. [91], and the comparison of some algorithms (TREMBLAY, VERNIORY, NAKAO) was compared. Also, the comparison of the results of simulations with experimental data was carried out by Verliefde and al. [89], and the pore flow-based models were compared with other models by Dijkstra and al. [84].

4.5 Donnan Equilibrium

Considering that most of the NF membrane has a negative surface charge, the equilibrium between the membrane and the solution appears when the membrane is in contact with the electrolyte solution. According to Williams [2], if it was assumed that the electrolyte in solution dissociates following the equation:

$$M_n N_m = M^{m+} + N^{n-} \tag{32}$$

then the dynamic equilibrium between the negatively charged membrane and the salt solution is established. In this case, the distribution coefficient can be represented in a form [2]:

$$K = \frac{C_{im}}{C_{Fi}} = \left[\left(\frac{n \cdot C_{Fi}}{C_m^*} \right)^n \left(\frac{\gamma}{\gamma_m} \right)^{m+n} \right]^{\frac{1}{m}} \tag{33}$$

where *C*im is the ions concentration in a membrane; C_{Fi} is the ions concentration in feed solution; C^*_m is the membrane charge capacity; γ is the activity coefficient of the ions in solution; γ_m – is the activity coefficient of the ions in the membrane

Based on Donnan equilibrium, the steric exclusion model was developed according to that the partitioning between the membrane and the bulk of solution can be represented in a form [92]:

$$\left(\frac{\gamma_i c_i}{\gamma_i^0 C_i} \right) = \Phi \exp\left(-\frac{z_i F}{RT} \Delta\Psi_D \right) \tag{34}$$

where γ_i is the activity coefficient of the ions in the membrane; γ^0_i is the activity coefficients in the bulk of the solution; C_i the concentration of the ions in the solution; Φ is the steric partitioning; z_i is the ion valence; F is the Faraday constant; R is the gas constant; T is the absolute temperature; $\Delta\Psi_D$ is the electric potentials difference.

From the Donnan equilibrium, the rejection rate of each solute can be obtained according to Szymczyk et al. [93] can be expressed in a form:

$$R_i = 1 - \frac{c_i\left(\Delta x^+\right)}{c_i\left(0^-\right)} \tag{35}$$

where $c_i\left(0^-\right)$ is the ions concentration on the entrance of the pore; $c_i\left(\Delta x^+\right)$ is the ions concentration on the output of the pore.

It should be noticed that Szymczyk and al. [93] wrote down the equilibrium on the entrance and output of the pores, and the equation (35) was modified with considering the solvation energy. Moreover, in many cases, the Donnan steric exclusion model was

supplemented by considering the dielectric exclusion [94–97].

Considering the assumption of the Donnan steric exclusion model, it was logical to applicate it for the electrolyte separation simulation [92–98], but this approach was also used for NF of organic compounds [99]. The Donnan equilibrium allows predicting the selectivity with high accuracy but does not show anything about the flux. Therefore, for the prediction of the flux through the charged membranes in most cases, it is used the extended Nernst-Plank equation, which is discussed in more detail below. For this reason, the Donnan steric exclusion model is often supplemented by the model based on this equation [92, 94, 98].

4.6 Extended Nernst–Plank equation

Hilal and al. [100] noticed in comprehensive review work that most NF models are based on the extended Nernst-Plank equation. This statement is in agreement with the data shown in Fig. 5.

According to Bowen and al. [101], the extended Nernst–Plank equation describes the transport of ions in the membrane pores by relationship as follows:

$$j_i = -D_{i,p}\frac{dc_i}{dx} - \frac{z_i c_i D_{i,p}}{RT} F \frac{d\psi}{dx} + K_{i,c} c_i V \qquad (36)$$

where $D_{i,p}$ is the diffusivity coefficient of the solute in pores; z_i is the valence of the ion; c_i is the concentration inside the membrane; R is the gas constant; T is the absolute temperature; F the Faraday constant; $K_{i,c}$ is the hindrance factor for convection of ion; V is the solvent velocity.

Also, Bowen and al. [101] pointed out that electroneutrality in the bulk of the solution and into the membrane can be written in a form:

$$\sum_{i=1}^{n} z_i C_i = 0 \qquad (37)$$

$$\sum_{i=1}^{n} z_i c_i = 0 \qquad (38)$$

where C_i is the concentration in bulk.

In equation (36), the first term describes the diffusion transport, the second one describes the transport by the electrostatic forces, and the third one describes the convective transport [2]. It should be noticed that Chaabane and al. [102] defined that, in the case of the NF od salt solutions, the dominant contribution to the flux belongs to convections.

Under conditions of the electrical neutrality in pores and the absence of the current equation (36) can be solved relatively to gradient potential [101]:

$$\frac{d\psi}{dx} = \frac{\sum_{i=1}^{n}\left(z_i V / D_{i,p}\right)\left(K_{i,c}c_i - C_{i,p}\right)}{\left(F/RT\right)\sum_{i=1}^{n} z_i^2 c_i} \qquad (39)$$

Similarly, the gradient potential can be represented in a form [101]:

$$\frac{dc_i}{dx} = \frac{V}{D_{i,p}}\left(K_{i,c}c_i - C_{i,p}\right) - z_i \frac{F}{RT} c_i \frac{d\psi}{dx} \qquad (40)$$

This approach allows solving the coupled equation using the numerical methods [101].

The selectivity of the process can be evaluated using the Donnan equilibrium described above. For the simplest case with include uncharged solutes, the simplified solution can be obtained [101]:

$$R_i = 1 - \frac{K_{i,c}\Phi_i}{1 - \left[1 - K_{i,c}\Phi_i\right]\exp\left(-Pe'\right)} \qquad (41)$$

where Φ_i is the steric partitioning coefficient; *Pe*' is the modified Peclet number.

In the period under consideration, the extended Nernst-Plank equation was applied primarily for the describing of salt solutions separation [92, 102–106], in particular for the water softening [107, 108]. It was also used for the cases of the isolation of the pharmaceuticals [109], the products of the fermentation [101], and surfactants [110].

It was mentioned above that the Spiegler–Kedem and solution-diffusion models were used for the determination of the membrane characteristics. The extended Nernst-Plank equation was also applied for these purposes in a case of charged membranes [82, 83]. Furthermore, the Teorell–Meyer Sievers method was used for the determination of the effective charge density.

In some researches for more accurate describing on NF process, the considered equation was supplemented by considering the additional factors. They include the Donnan equilibrium [94, 98, 108, 109], the Born exclusion [109], the adsorption [110], the energy of solvation [108], and the concentration polarization [103].

The comparison of the models based on the extended Nernst-Plank equation with the other models [76, 81-83, 94] shows that this model in mist suitable for the description of the electrolyte solutions separation, whereas Mandale and Jones [81] claimed that the Spiegler–Kedem model is more suitable for the describing if the NF of the organic compound solutions. Although Wendler and al. [110] pointed out that the extended Nernst–Plank equation was valid for the case of the sodium dodecyl sulfate solution separation, moreover, another disadvantage limitation of the considered in the current section approach is the inaccuracy of the assumption about the equality of the surface charge and the charge into the membrane [109]. In this case, the incorporation of the fitted parameter is recommended for compensation of this disagreement [109].

4.7 Maxwell–Stephan equations

The use of the Maxwell-Stephan equations is another approach to the NF simulation, which considers the membrane charge. According to Noordman and Wesselingh [111], this transport equation can be characterized as a force balance on the individual

components of the mixture. In other words, the sum of the driving force on the particle i is equal to the frictions with all other particles *j*.

The other assumption of these equations is that the friction force by any particle j on the particle i is proportional to the friction of j in the mixture, and also, this force is proportional to the difference in velocities between two particles. The simplest case is a liquid mixture since it can be considered as homogenous on a small scale (if the chosen elementary volumes are much bigger than the molecule dimensions) [111].

Under isothermal conditions, the Maxwell-Stephan equations can be written in a form [111]:

$$F_i = \sum_j x_j \zeta_{i,j} \left(u_i - u_j\right) \tag{42}$$

where x_j is the particle *j* concentration (molar fraction); $\zeta_{i,j}$ is the friction coefficient between particles *i* and *j*; u_i and u_j are the diffusive volumetric fluxes of the particle *i* and *j* correspondingly.

The driving force is the gradient of the electrochemical potential of the *i*-th component of the mixture. In most cases, it can be represented as a sum of the gradients of the chemical potential, pressure, and electrical potential [111]:

$$F_i = -\nabla_p \mu_i - V_i \nabla P - z_i F \nabla \Psi \tag{43}$$

where $\nabla_p \mu_i$ is the gradient of the chemical potential of the particle *i* in the membrane pores; V_i is the partial molar volume of the particle *i*; ∇P is the pressure gradient; z_i is the valence of the ion; F is the Faraday constant; $\nabla \Psi$ is the electrical potential gradient.

If the dimensions of all parameters are in the SI system, the driving force is expressed in Newtons per mole [111].

Under idealized conditions which include the consideration of the distribution of the small spherical particles in viscous liquids, the friction coefficient can be defined from Stokes law [111]:

$$\zeta_{i,j} = L_a 3\pi\eta d_i \tag{44}$$

where L_A is the Avogadro number; η –is the dynamic viscosity; d_i is the particle diameter.

It should be noticed that in liquids, the friction coefficients for the two particles are equal [111]:

$$\zeta_{i,j} = \zeta_{j,i} \tag{45}$$

Equation (45) is known as the Onsager reciprocal relation [111].

Considering (43), equation (42) also can be rewritten in specific parameters (in terms per mole of the mixture) [111]:

$$x_i\left(-\nabla_p \mu_i - V_i \nabla P - z_i F \nabla \Psi\right) = \sum_j x_i x_j \zeta_{i,j} \left(u_i - u_j\right) \tag{46}$$

Moreover, the friction coefficient can be replaced by the Maxwell–Stefan diffusivity coefficients [111]:

$$D_{i,j} = \frac{RT}{\zeta_{i,j}} \tag{47}$$

To define the overall volumetric flux, the viscous flux of the mixture should be added to diffusion flux [111]:

$$w_i = u_i + v_f \tag{48}$$

The Maxwell-Stephan equations, therefore, allow defining the velocity profile in the membrane pores and, consequently, the values of the fluxes. The effectivity of the separation, according to this approach, can be evaluated, for example, by using the viscous selectivity value. This parameter can be represented in a form [111]:

$$\alpha_i = \frac{\left(2 - \phi_i\right) K_s}{2K_t} \tag{49}$$

where φ_i, K_s, K_t the coefficients, which depend on the pore size of the membrane and the solute properties.

The models based on the Maxwell-Stephan appeared to be suitable for the description of the transport of the organic compound, including organic solvents [84, 112] and also for the simulation of the separation of the multicomponent mixture [113]. For the case of the salt solution, this approach is suitable for the description of the transport through the ceramic membranes [114].

It should be noticed that the Spiegler–Kedem model and the extended Nernst-Plank equation can be considered as a particular case of the Maxwell-Stephan equations [111].

4.8 Computational fluid dynamics

The extended Nernst–Plank equation allows adequately describing of the NF process, unlike the case of reverse osmosis, there is no entirely necessary to use the methods of computational fluid dynamics. However, some papers about this kind of NF simulation were published. Most of them were carried out by one research group, including Geraldes, Semiao, and de Pinho [115–117] without using commercially available software. The coupled equations (equation (29)–(31)) were solved using the finite volume method. In the mentioned set of researches, the primary attention was dedicated to the salt solution separation. They considered both diffusive and convective transport and also the transport of matter insight into the membrane and the solute-membrane interactions (the las factors were considered in boundary conditions of mass transfer). The investigations were carried out for the cell, which simulates the spiral wound module, and experiments verified the results. The same cell was considered by Koutsou and al. [35] using commercial software Fluent. It this work, the influence of spacers, hydrodynamic conditions, and solute properties was considered. Mentioned above factors were considered by spacer angles (Fig. 4), Reynolds number (Re), and Schmidt number (Sc).

4.9 Artificial neural networks

It was mentioned above that the application of the ANN is rational when the nature of the phenomena is not clearly understood. At the same time, during the simulation of the NF, the physical phenomena are reasonably

comprehensive, considered by the discussed above models. Therefore, in the considered period, the artificial neural network was not widely used. In some researches, this approach was applied to the simulation of the separation of multicomponent mixtures [118] and organic compounds [119], and of the water treatment [26, 79]. The separation of the multicomponent systems is the most suitable case of ANN application since, in that case, the process selectivity is characterized by nonlinear dependences on the concentration of components, applied pressure, and pH [118]. In such conditions, the simulation-based on physical principles is complicated. Despite that ANN are more effective that the solution-diffusion model [26] and is in good agreement with experimental data (the difference was in the range of 5–8 %) [79], this approach was used in a limited range.

4.10 Optimization and economic analysis

As in a case of reverse osmosis, the determination of the optimal conditions for the process performance is a significant question for the practical application of the NF. For optimization of the NF process, the methods similar to ones described in section 3.7 were used.

In most cases, the economic parameters have been accepted as optimal criteria, including the minimum capital and energy requirements [87, 120–122] and also the maximal annual profit [123]. The optimization procedure also was carried out to minimize the level of fouling (using the conception of the critical flux) [124] and to define the optimal characteristics of membranes, including porosity and surface charge [125]. It should be noticed that Yaroshchuk [125] claimed that the characteristics of the conventional NF membrane do not correspond to the optimal conditions.

The optimization of the NF was carried out using the phenomenological equations [87], the extended Nernst-Plank equations [101, 126], artificial neural networks [118], and also the factor experiment methods [67]. In general, the same approaches, as in the case of RO, were used.

4.11 Other approaches to simulation of nanofiltration

In some cases, the other approaches to the simulation of the NF process were used. First of all, this relates to the specific systems, such as diafiltration set-ups [127] and composite membranes with a catalyst layer [128], where the conventional models are not suitable. There are also cases when tits rational to use simplified [129, 130] and semi-empirical approaches [131–135], or otherwise when it is necessary to consider the imperfections [136, 137]. Moreover, since the NF membranes are electrically charged, the models for calculation of the surface charge were developed [138, 139].

5 Ultrafiltration

5.1 Classification of ultrafiltration models

The simulation of the UF process is based on the same approaches as reverse osmosis (Fig. 6). However, since UF membranes have pores up to 0.1 μm [140], the models based on the diffusion almost were not applied. Only Das and De [86], which considered the treatment of the effluent collected from a tannery by consistent NF and UF, used the solution-diffusion model for the description of both processes.

The irreversible thermodynamics also used only in particular cases, for example, Wang and Rodgers [141] considered the model, based on the Kedem–Katchalsky approach, and Katsikaris and al. [140] took the Spiegler–Kedem model as a basis. It should be noticed that in both cases, the separation of natural polymers, including proteins, and the models were supplemented by additional terms that consider the concentration polarization.

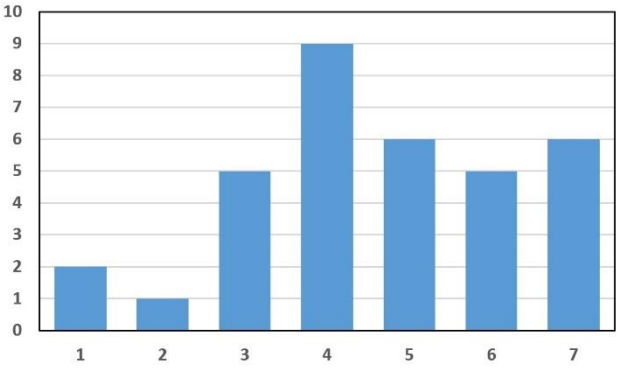

Figure 6 – The number of NF models in the chosen articles by classes: 1 – models based on irreversible thermodynamics; 2 – models based on diffusion, 3 – models based on pore flow; 4 – models based on CFD; 5 – models based on ANN; 6 – optimization; 7 – other models.

Since the number of these models is small, it is not reasonable to make them a separate section.

It also should be noticed that the relative number of models based on artificial neural networks for UF is more significant than for RO and NF.

5.2 Pore flow-based models

Unlike the RO model, in which both diffusive and convective mechanisms of transport are considered and the models themselves based on the force balance (in the case of NF, the electrostatic relationships are also considered), in the case of UF, the more straightforward approaches are used. They are based on the Darcy equation and the Hagen–Poiseuille equation. This is due to the more significant dimensions of pores in UF membranes.

The Darcy equation can be written in a form [142]:

$$V_p = \frac{P}{\mu\left(R_m + r_c\Gamma\right)} \qquad (50)$$

where V_p is the specific volumetric productivity by permeate; P is the transmembrane pressure; μ is the viscosity of liquid; R_m is the clean membrane resistance; r_C is the specific cake resistance; Γ – specific cake deposit (cake mass per unit membrane shell surface area) [142].

It should be noticed that in equation (50), unlike conventional filtration, the cake resistance is not

determined using its thickness. For this purpose, the specific parameter Γ has been introduced. This characteristic can be defined from the mass conservation equation. For the case of the hollow-fiber membranes, it was represented by Polyakov[142] in a form:

$$\frac{\partial c}{\partial t} + \frac{\partial (cw)}{\partial z} = -s\frac{\partial \Gamma}{\partial t} \quad (51)$$

where c is the solute concentration (for the case of microfiltration, this is the concentration of the suspended particles); t is the time; z is the coordinate normal to the length of the hollow fiber; w is the fluid velocity; s is the specific membrane surface.

The joint solution of the equation (50) and equation (51) can be defined for the cases of constant pressure and constant permeate flux [142].

The Darcy equation appears to be useful for the development of artificial neural networks [143].

The Hagen–Poiseuille equation is a form of expression of the momentum balance for a case of the laminar flow in capillaries. In can be written for the tubular modules in a form [144]:

$$-\frac{d\Delta p}{dz} = \frac{8\mu Q}{\pi r_m^4 F} \quad (52)$$

where Δp is the transmembrane pressure; μ is the viscosity of solution; Q is the volumetric flow rate; r_m is the membrane channel radius; F is the correction factor.

However, usually, the Hagen–Poiseuille equation requires the corrections, for example, considering the concentration polarization and resistances to mass transfer [144, 145]. It is rational to use the numeric methods, including the finite element method, for the solution of these models [146].

5.3 Computational fluid dynamics

For the case of UF, the CFD methods were more frequently used than for NF. In this case, the same commercial software, such as ANSYS [45] and FLUENT [147-150], was applied. The Comsol [151] and the realization of computational algorithms without the commercial program products [152-154] were also used.

The simulation using the CFD was mainly applied to the solving of the common problems of the UF, which are related to the concentration of macromolecular compounds, including proteins [151], bovine serum albumin [152, 154], and oil-water emulsions [153]. Among the nonconventional approaches, the researches, which deserves attention, include the gas injection in the stream of feed solution [149] and the detailed analysis of the vortex formation in membrane channels [147, 148].

The specifics of the UF process require paying more attention to the concentration polarization phenomena [45, 151], the gel layer formation [154], and the adsorption of the feed solution components by the membrane material [154]. Also, the influence of the concentration on the values of the viscosity, osmotic pressure, and diffusivity are more significant in comparison with other processes [45, 152]. Therefore, as it was pointed out by Wiley and Fletcher [45], the excessive simplification of the dependencies of these values on concentration leads to the misleading obtained in simulation.

5.4 Artificial neural networks

The wide range of use of ANN for the simulation of the UF process is likely explained by the more significant influence of concentration polarization and the more significant tendency to the fouling formation in comparison with RO and NF. To confirm this assumption that the questions of concertation polarization and fouling are involved in most models of this class [143, 155–158]. The ANNs were also a useful tool for describing the UF realization in the pulsation mode [155, 159].

This approach to simulation was used for the application of UF in the drinking water production from surface waters [143, 156], the concentrating of bovine serum albumin [155, 159], and the separation of milk [157, 158]. Artificial neural networks were designed based on both only experimental data [156, 157, 159] and theoretical understanding [143, 155]. It was pointed out by Curcio et al. [159] that the results of simulation by ANN were in good agreement with the experimental data, and differences were less than 5 %.

5.5 Optimization

The number of articles dedicated to the optimization of the UF is somewhat less in comparison with the described above processes. The probable reason for this is a more significant influence of concentration polarisation, which was mentioned in sections 5.3 and 5.4. In these conditions, the optimization problem becomes more complicated.

Such parameters as the minimal membrane surface area [160], the maximal profit [123], and minimal cost of the membrane (by the determination of the optimal duration of the operation time of membrane) [161] were chosen as optimal criteria. The optimization procedure was also carried out for the cleaning cycles [162] and the membrane manufacturing [163] (the optimization was aimed at the determination of the conditions, which provide the integrity of the skin layer). The optimization was carried out for the case of wastewater treatment [123, 162] and the concentration of the dairy products [160].

5.6 Other approaches to simulation of ultrafiltration

It was pointed out by Paris and al. [164] that conventional models, in particular, the gel layer model or osmotic pressure model give the results, which are not in agreement with the experimental data. Therefore, in this work, the new model was developed. It can be considered as close to the CFD approach. Similar models based on the mass and momentum balances were developed by Sarkar and al. [165] and Yeh and Chen [166]. Moreover, the models based on dimensionless equations for determination of mass transfer coefficient [167] and chemical kinetics [168] were used. In most cases, such models were applied to the unique systems, including the stirring cells [165], the presence of the wired-rod insight the membrane channel [166], and the hybrid process, which includes the chelating and ultrafiltration [168].

As in most considered above cases, during the simulation of the UF, the unconventional models consider the concentration polarization and fouling [164, 166, 167], in particular the influence of the properties of the contaminants (including the rheological properties) on the transport intensity [169].

6 Microfiltration and other processes

The MF process is close to UF by its physical essence, therefore for the simulation of both processes the similar approaches are applied, including Darcy and Hagen–Poiseuille equations [170] and the CFD methods [171]. The UF and MF are similar by being influenced by the concentration polarization, which is considered in both mentioned researches.

It should be noticed that MF and sometimes UF is often used in the membrane bioreactors, which are used for the biological wastewater treatment [172]. The membrane bioreactors are the membrane units (usually hollow-fiber ones), immersed in the vessel, in which the wastewater and active sludge are supplied [172]. The simulation of the membrane processes in that systems can be carried out using the conventional for the MF methods, including the Darcy equation [170, 172] and Hagen–Poiseuille equation [170], and also with using of the optimization methods [173].

The forward osmosis also belongs to the pressure-driven membrane processes. For the description of this process, the osmotic pressure model is the most often used. According to it, the permeate flux can be represented in a form [174]:

$$J_w = A\left(\pi_{d.w} - \pi_{f,w}\right) \tag{53}$$

where A is the penetration constant for the clean water; $\pi_{d.w} - \pi_{f,w}$ is the effective osmotic pressure difference.

This model also should be supplemented by terms, considering the concentration polarization. Moreover, both types of concentration polarization, namely diluted (at the permeate side) and concentrated (at the feed side), should be considered [174]. Additionally, it should be noticed that in some works, the models of the membrane manufacturing processes [163, 175, 176] and the estimation of its properties [177, 178] were developed.

7 Conclusions

In the present article, the published researches dedicated to the mathematical modeling of the pressure-driven membrane processes for the period 2000–2010 was reviewed and analyzed. The key positions are following: (i) except the conventional approaches (including irreversible thermodynamics, diffusion, and fore flow) the novel methods found full application including primarily CFD methods and also the artificial neural networks and optimization methods; (ii) the irreversible thermodynamics and the diffusion approaches was still used to a limited extend for the analysis of RO and NF processes in cases when there was not necessary for high accuracy of predicting, and also for the characterization of the novel membranes. This is due to the relative simplicity of such models; (iii) in the earlier reviews [1, 2] it was pointed out that preferential sorption-capillary flow model was the most widely used model of RO process, but in the period under consideration, it was used by a relatively low number of the researches. Instead, the CFD method was used on larger scales. Considering the development of the computer technologies, it is reasonable to assume that this is the most perspective way in the simulation of all pressure-driven membrane processes; (iv) the extended Nernst-Plank equation is the most effective way for the simulation of NF. It describes the all physical phenomena involved, which take place in this process, with reasonable completeness; (v) the Darcy and Hagen–Poiseuille equations are the most suitable approach for the simulation of UF and MF; (vi) despite that the artificial neural networks can be more accurate in predictions than physically based models, its application was limited, and the most reasonable cases for using this approach are processes with significant influence of the concentration polarization and fouling formation; (vii) the optimization of the pressure-driven membrane processes in most cases was based on the optimal economic criteria, including the minimal energy consumption for the process performance; (viii) in most cases for the destination the comprehension of the mathematical description of the process, the transport models should be supplemented by terms with considers the concentration polarization.

This conclusion allows for estimating the development of the simulation of pressure-driven membrane processes more thoroughly. Moreover, even at this stage, the current review allows choosing the most suitable strategy for the simulation of pressure-driven membrane processes.

References

1. Soltanieh M., Gill W. (1981). Review of reverse osmosis membranes and transport models, *Chemical Engineering Communications*, 12, pp. 279-363, doi: 10.1080/00986448108910843.
2. Williams M. (2003). A Review of Reverse Osmosis Theory. Available at http://docplayer.net/33542358-A-review-of-reverse-osmosis-theory-michael-e-williams-ph-d-p-e.html. (Acceded: 13.03.2019).
3. Sobana S., Panda R. C. (2011). Review on modeling and control of desalination system using reverse osmosis, *Reviews in Environmental Science and Bio/Technology*, 10 (2), pp. 139–150, https://doi.org/10.1007/s11157-011-9233-z.

4. Jarzynska M. (2005) Mechanistic equations for membrane substance transport are consistent with Kedem–Katchalsky equations, *Journal of Membrane Science*, 263, pp.162–163, https://doi.org/10.1016/j.memsci.2005.07.016.
5. Koter S. (2005). The Kedem-Katchalsky equations and the sieve mechanism of membrane transport, Journal of Membrane Science, 246, pp. 109–111. https://doi.org/10.1016/j.memsci.2004.08.022.
6. Kargol A. (2000.). Modified Kedem-Kathcalsky equations and their applications, *Journal of Membrane Science*, 174, pp. 43–53, https://doi.org/10.1016/S0376-7388(00)00367-7.
7. Kargol M., Kargol A. (2003). Mechanistic equations for membrane substance transport and their identity with Kedem–Katchalsky equations, *Biophysical Chemistry*, 103, pp. 117–127, https://doi.org/10.1016/S0301-4622(02)00250-8.
8. Slezak A., Grzegorczyn S., Wasik J. (2004). Model equations for interactions of hydrated species in transmembrane transport" *Desalination*, 163, pp. 177-192, https://doi.org/10.1016/S0011-9164(04)90188-9.
9. Pontié M., Dach H., Leparc J., Hafsid M., Lhassani A. (2008). Novel approach combining physico-chemical characterizations and mass transfer modelling of nanofiltration and low pressure reverse osmosis membranes for brackish water desalination intensification, *Desalination*, 221, pp. 174–191, https://doi.org/10.1016/j.desal.2007.01.075.
10. Villafafila A., Mujtaba I.M. (2003). Fresh water by reverse osmosis based desalination: simulation and optimisation, *Desalination*, 155, pp. 1-13, https://doi.org/10.1016/S0011-9164(03)00234-0.
11. Hyung H., Kim J.-H. (2006). A mechanistic study on boron rejection by sea water reverse osmosis membranes, *Journal of Membrane Science*, 286, pp. 269–278, https://doi.org/10.1016/j.memsci.2006.09.043.
12. Senthilmurugan S., Ahluwalia A., Gupta S. (2005). Modeling of a spiral-wound module and estimation of model parameters using numerical techniques, *Desalination*, 173, pp. 269-286,. https://doi.org/10.1016/j.desal.2004.08.034.
13. Al-haj Ali M., Ajbar A., Ali E., Alhumaizi K. (2009) Modeling the transient behavior of an experimental reverse osmosis tubular membrane, *Desalination*, 245, pp. 194-204, https://doi.org/10.1016/j.desal.2008.06.019.
14. Chatterjee A., Ahluwalia A., Senthilmurugan S., Gupta S. K. (2004). Modeling of a radial flow hollow fiber module and estimation of model parameters using numerical techniques, *Journal of Membrane Science*, 236, pp. 1–16, 2004. https://doi.org/10.1016/j.memsci.2004.01.006.
15. Senthilmurugan S., Gupta S. (2006) Modeling of a radial flow hollow fiber module and estimation of model parameters for aqueous multi-component mixture using numerical techniques, *Journal of Membrane Science*, 279, pp. 466–478, https://doi.org/10.1016/j.memsci.2005.12.041.
16. Mane P., Park P.-K., Hyung H., Brown J., Kim J.-H. (2009) Modeling boron rejection in pilot- and full-scale reverse osmosis desalination processes, *Journal of Membrane Science*, 338, pp. 119–127, https://doi.org/10.1016/j.memsci.2009.04.014.
17. Jain S., Gupta S. K. (2004). Analysis of modified surface force pore flow model with concentration polarization and comparison with Spiegler–Kedem model in reverse osmosis systems, *Journal of Membrane Science*, 232, pp. 45–61, https://doi.org/10.1016/j.memsci.2003.11.021.
18. Moresi M., Ceccantoni B., Lo Presti S. (2002) Modelling of ammonium fumarate recovery from model solutions by nanofiltration and reverse osmosis, *Journal of Membrane Science*, 209, pp. 405–420, https://doi.org/10.1016/S0376-7388(02)00330-7.
19. Ahmad A.L., Chong M.F., Bhatia S. (2007) Mathematical modeling of multiple solutes system for reverse osmosis process in palm oil mill effluent (POME) treatment, *Chemical Engineering Journal*, 132, pp. 183–193, https://doi.org/10.1016/j.cej.2006.12.022.
20. Yaroshchuk A. (2002) Rejection of single salts versus transmembrane volume flow in RO/NF: thermodynamic properties, model of constant coefficients, and its modification, *Journal of Membrane Science*, 198, pp. 285–297, https://doi.org/10.1016/S0376-7388(01)00668-8.
21. Bhanushali D., Kloos S., Kurth C., Bhattacharyya D. (2001) Performance of solvent-resistant membranes for non-aqueous systems: solvent permeation results and modeling, *Journal of Membrane Science*, 189, pp. 1–21, https://doi.org/10.1016/S0376-7388(01)00356-8.
22. Sagne C., Fargues C., Broyart B., Lameloise M.-L., Decloux M. (2009). Modeling permeation of volatile organic molecules through reverse osmosis spiral-wound membranes, *Journal of Membrane Science*, 330, pp. 40–50,. https://doi.org/10.1016/j.memsci.2008.12.038.
23. Avlonitis S. A., Pappas M., Moutesidis K. (2007) A unified model for the detailed investigation of membrane modules and RO plants performance, *Desalination*, 203, pp. 218–228, https://doi.org/doi/10.1016/j.desal.2006.04.009.
24. Kaghazchi T., Mehri M., Ravanchi M. T., Kargari A. (2010). A mathematical modeling of two industrial seawater desalination plants in the Persian Gulf region, *Desalination*, 252, pp. 135–142, https://doi.org/doi/10.1016/j.desal.2009.10.012.
25. Oh. H.-J., Hwang T.-M., Lee S. (2009) A simplified simulation model of RO systems for seawater desalination, *Desalination*, 238, pp. 128-139,. https://doi.org/10.1016/j.desal.2008.01.043.
26. Zhao Y., Taylor J., Chellam S. (2005) Predicting RO/NF water quality by modified solution diffusion model and artificial neural networks, *Journal of Membrane Science*, 263, pp. 38–46, https://doi.org/10.1016/j.desal.2008.01.043.
27. Yaroshchuk A. (2010)/ Influence of osmosis on the diffusion from concentrated solutions through composite/asymmetric membranes: Theoretical analysis, *Journal of Membrane Science*, 355, pp. 98–103, 2010. https://doi.org/10.1016/j.memsci.2010.03.013.
28. Mehdizadeh H., Molaiee-Nejad Kh., Chong Y.C. (2005). Modeling of mass transport of aqueous solutions of multi-solute organics through reverse osmosis membranes in case of solute–membrane affinity Part 1. Model development and simulation, *Journal of Membrane Science*, 267, pp. 27–40, https://doi.org/10.1016/j.memsci.2005.03.059.

29. Kumano A, Sekino M., Matsui Y., Fujiwara N., Matsuyama H. (2008) Study of mass transfer characteristics for a hollow fiber reverse osmosis module, *Journal of Membrane Science*, 324, pp. 136–141, https://doi.org//10.1016/j.memsci.2008.07.011.
30. Weissbrodt J., Manthey M., Ditgens B., Laufenberg G, Kunz B. (2001) Separation of aqueous organic multi-component solutions by reverse osmosis – development of a mass transfer model, *Desalination*, 133, pp. 65-74, https://doi.org/10.1016/S0011-9164(01)00083-2.
31. Sreenivas K., Ragesh P., DasGupta S., De S. (2002). Modeling of cross-flow osmotic pressure controlled membrane separation processes under turbulent flow conditions, *Journal of Membrane Science*, 201, pp. 203–212, https://doi.org/10.1016/S0376-7388(01)00730-X.
32. Koutsou C.P., Yiantsios S.G., Karabelas A.J. (2004). Numerical simulation of the flow in a plane-channel containing a periodic array of cylindrical turbulence promoters, *Journal of Membrane Science*, 231, pp. 81–90,. https://doi.org/10.1016/j.memsci.2003.11.005.
33. Ghidossi R., Veyret D., Moulin P. (2006). Computational fluid dynamics applied to membranes: State of the art and opportunities, *Chemical Engineering and Processing*, 45, pp. 437–454, https://doi.org/10.1016/j.cep.2005.11.002.
34. Ahmad A.L., Lau K.K. (2006). Impact of different spacer filaments geometries on 2D unsteady hydrodynamics and concentration polarization in spiral wound membrane channel, *Journal of Membrane Science*, 286, pp. 77–92, https://doi.org/10.1016/j.memsci.2006.09.018.
35. Koutsou C.P., Yiantsios S.G., Karabelas A.J. (2009). A numerical and experimental study of mass transfer in spacer-filled channels: Effects of spacer geometrical characteristics and Schmidt number, *Journal of Membrane Science*, 326, pp. 234–251, https://doi.org/10.1016/j.memsci.2008.10.007.
36. Lau K.K., Abu Bakar M.Z., Ahmad A.L., Murugesan T. (2009). Feed spacer mesh angle: 3D modeling, simulation and optimization based on unsteady hydrodynamic in spiral wound membrane channel, *Journal of Membrane Science*, 343, pp. 16–33, https://doi.org/10.1016/j.memsci.2009.07.001.
37. Li Y.-L., Tung K.-L. (2004). CFD simulation of fluid flow through spacer-filled membrane module: selecting suitable cell types for periodic boundary conditions, *Desalination*, 233, pp. 351–358, https://doi.org/10.1016/j.desal.2007.09.061.
38. Shakaib M., Hasani S.M.F., Mahmood M. (2007) Study on the effects of spacer geometry in membrane feed channels using three-dimensional computational flow modeling, *Journal of Membrane Science*, 297, pp. 74–89, https://doi.org/10.1016/j.memsci.2007.03.010.
39. Ranade V., Kumar A. (2006) Fluid dynamics of spacer filled rectangular and curvilinear channels, *Journal of Membrane Science*, 271, pp. 1–15, https://doi.org/10.1016/j.memsci.2005.07.013.
40. Alexiadis A., Wiley D.E., Vishnoi A., Lee R.H.K., D.F. Fletcher, Bao J. (2007) CFD modelling of reverse osmosis membrane flow and validation with experimental results, *Desalination*, 217, pp. 242–250, 2007. https://doi.org/10.1016/j.desal.2007.02.014.
41. Fimbres-Weihs G.A., Wiley D.E. (2007) Numerical study of mass transfer in three-dimensional spacer-filled narrow channels with steady flow, *Journal of Membrane Science*, 306, pp. 228–243, https://doi.org/10.1016/j.memsci.2007.08.043.
42. Li F., Meindersma W., de Haan A.B., Reith T. (2002). Optimization of commercial net spacers in spiral wound membrane modules, Journal of Membrane Science, 208 pp. 289–302, https://doi.org/10.1016/S0376-7388(02)00307-1.
43. Li F., Meindersma W., de Haan A.B., Reith T. (2004). Experimental validation of CFD mass transfer simulations in flat channels with non-woven net spacers, *Journal of Membrane Science*, 232, pp. 19–30, 2004. https://doi.org/10.1016/j.memsci.2003.11.015.
44. Schwinge J., Wiley D.E., Fletcher D.F. (2002). A CFD study of unsteady flow in narrow spacer-filled channels for spiral-wound membrane modules, *Desalination*, 146, pp. 195-201, https://doi.org/10.1016/S0011-9164(02)00470-8.
45. Wiley D., Fletcher D. (2003). Techniques for computational fluid dynamics modelling of flow in membrane channels, *Journal of Membrane Science*, 211, pp. 127–137,. https://doi.org/10.1016/S0376-7388(02)00412-X.
46. Ma S., Song L. (2006). Numerical study on permeate flux enhancement by spacers in a crossflow reverse osmosis channel, *Journal of Membrane Science*, 284, pp. 102–109,. https://doi.org/10.1016/j.memsci.2006.07.022.
47. Miyatake O., Tagawa K. (2001). Numerical and experimental analyses for RO desalination systems using a static pressure head, Desalination, 136, pp. 233-242, https://doi.org/10.1016/S0011-9164(01)00186-2.
48. Guo Y., Shi Y., Moncur J., Lee Y. T., Kime K. W., Kim A. S. (2010). Analysis of full-scale membrane filtration processes using econophysics and econometrics, *Journal of Membrane Science*, 365, pp. 170–179, https://doi.org/10.1016/j.memsci.2010.09.009.
49. Lee G.L., Lee Y.S., Jeon J.J., Lee S., Yang D.R., Kim I.S., Kim J.H. (2009). Artificial neural network model for optimizing operation of seawater reverse osmosis desalination plant, *Desalination*, 247, pp. 180-189, https://doi.org/10.1016/j.desal.2008.12.023.
50. Libotean D., Giralt J., Giralt F., Rallo R., Wolfe T., Cohen Y. (2009). Neural network approach for modeling the performance of reverse osmosis membrane desalting, *Journal of Membrane Science*, 326, pp. 408–419,. https://doi.org/10.1016/j.memsci.2008.10.028
51. Al-haj Ali M., Ajbar A., Ali E., Alhumaizi K. (2010). Robust model-based control of a tubular reverse-osmosis desalination unit, *Desalination*, 255, pp. 129–136, https://doi.org/10.1016/j.desal.2010.01.003.
52. Gotor A., De la Nuez Pestana I., Espinoza C. A. (2003). Optimization of RO desalination systems powered by renewable energies, *Desalination*, 156, p. 351, https://doi.org/10.1016/S0011-9164(03)00366-7.
53. Zilouchian A., Jafar M. (2001). Automation and process control of reverse osmosis plants using soft computing methodologies, *Desalination*, 135, pp. 51-59, https://doi.org/10.1016/S0011-9164(01)00138-2.

54. Gasmi A., Belgaieb J., Hajji N. (2010). Technico-economic study of an industrial reverse osmosis desalination unit, Desalination, 261, pp. 175–180, https://doi.org/10.1016/j.desal.2010.04.060.
55. Manth T., Gabor M., Oklejas E. (2003). Minimizing RO energy consumption under variable conditions of operation, *Desalination*, 157, pp. 9-21, https://doi.org/10.1016/S0011-9164(03)00377-1.
56. Calì G., Fois E., Lallai A., Mura G. (2008). Optimal design of a hybrid RO/MSF desalination system in a non-OPEC country, *Desalination*, 228, pp. 114–127, https://doi.org/10.1016/j.desal.2007.08.012.
57. Glueckstem P., Priel M. (2003). Optimization of boron removal in old and new SWRO systems, *Desalination*, 156, pp 219-228, https://doi.org/10.1016/S0011-9164(03)00344-8.
58. Helal A.M., El-Nashar A.M., Al-Katheeri E., Al-Malek S. (2003). Optimal design of hybrid RO/MSF desalination plants Part I: Modeling and algorithms", *Desalination*, 154, pp. 43-66, https://doi.org/10.1016/S0011-9164(03)00207-8.
59. Kim Y.M., Kim S.J., Kim Y.S., Lee S., Kim I.S., Kim J.H. (2009). Overview of systems engineering approaches for a large-scale seawater desalination plant with a reverse osmosis network, *Desalination*, 238, pp. 312-332, https://doi.org/10.1016/j.desal.2008.10.004.
60. Wilf M., Klinko K. (2001). Optimization of seawater RO systems design, *Desalination*, 138, pp. 299–306,. https://doi.org/10.1016/S0011-9164(01)00278-8.
61. Helal A.M., El-Nashar A.M., Al-Katheeri E.S., Al-Malek S.A. (2004). Optimal design of hybrid RO/MSF desalination plants Part II: Results and discussion, *Desalination*, 160, pp. 13-27, https://doi.org/10.1016/S0011-9164(04)90014-8.
62. Chilyumova E., Thöming J. (2007). Dynamic simulation of rinsing and regeneration networks based on high pressure RO, *Desalination*, 207, pp. 45–58, https://doi.org/10.1016/j.desal.2006.07.004.
63. Roth E., B., Accary A., Thomas G. (2000). Modelling of stimulus response experiments in the feed channel of spiral-wound reverse osmosis membranes, *Desalination*, 127, pp. 69-77, https://doi.org/10.1016/S0011-9164(99)00193-9.
64. Khayet M., Essalhi M., Armenta-Déu C., Cojocaru C., Hilal N. (2010). Optimization of solar-powered reverse osmosis desalination pilot plant using response surface methodology, *Desalination*, 261, pp. 284–292, https://doi.org/10.1016/j.desal.2010.04.010.
65. Jamal K., Khan M.A., Kamil M. (2004). Mathematical modelling of reverse osmosis systems, *Dessalination*, 160, pp. 29-42, https://doi.org/10.1016/S0011-9164(04)90015-X.
66. Stover R. (2008). SWRO process simulator, *Desalination*, 221, pp. 126–135, https://doi.org/10.1016/j.desal.2007.02.049.
67. Peng W., Escobar I., White D. (2004). Effects of water chemistries and properties of membrane on the performance and fouling – a model development study, *Journal of Membrane Science*, 238, pp. 33–46, https://doi.org/10.1016/j.memsci.2004.02.035.
68. Avlonitis S.A., Kouroumbas K., Vlachakis N. (2003). Energy consumption and membrane replacement cost for seawater RO desalination plants, *Desalination*, 157, pp. 151-158, https://doi.org/10.1016/S0011-9164(03)00395-3.
69. Nafey A.S., Sharaf M.A , García-Rodríguez L. (2010). Thermo-economic analysis of a combined solar organic Rankine cycle-reverse osmosis desalination process with different energy recovery configurations, *Desalination*, 261, 138–147, https://doi.org/10.1016/j.desal.2010.05.017.
70. Park C., Park P.-K., Manec P., Hyungc H., Gandhi V., Kim S.-H., Kim J.-H. (2010). Stochastic cost estimation approach for full-scale reverse osmosis desalination plants, *Journal of Membrane Science*, 364, pp. 52–64, https://doi.org/10.1016/j.memsci.2010.07.055.
71. Majali F., Ettouney H., Abdel-Jabbar N., Qiblawey H. (2008). Design and operating characteristics of pilot scale reverse osmosis plants, *Desalination*, 222, pp. 441–450, https://doi.org/10.1016/j.desal.2007.01.169.
72. van Gauwbergen D., Baeyens J. (2001). Modelling and scale-up of reverse osmosis separation, *Desalination*, 139, p. 275, https://doi.org/10.1016/S0011-9164(01)00319-8.
73. Cheddie D., Maharajh A., Ramkhalawan A., Persad P. (2010). Transient modeling of wave powered reverse osmosis, Desalination, 260, pp. 153–160, https://doi.org/10.1016/j.desal.2010.04.048.
74. Zhou W., Song L., Guan T. K. (2006). A numerical study on concentration polarization and system performance of spiral wound RO membrane modules, *Journal of Membrane Science*, 271, pp. 38–46, https://doi.org/10.1016/j.memsci.2005.07.007.
75. Ramon G., Agnon Y., Dosoretz C. (2010). Dynamics of an osmotic backwash cycle, *Journal of Membrane Science*, 364, pp. 157–166, https://doi.org/10.1016/j.memsci.2010.08.008.
76. Ahmad A.L., Chong M.F., Bhatia S. (2005). Mathematical modeling and simulation of the multiple solutes system for nanofiltration process, *Journal of Membrane Science*, 253, pp. 103–115, https://doi.org/10.1016/j.memsci.2005.01.005.
77. Kovács Z., Discacciati M., Samhaber W. (2009). Modeling of batch and semi-batch membrane filtration processes, *Journal of Membrane Science*, 327, pp. 164–173,. https://doi.org/10.1016/j.memsci.2008.11.024.
78. Kovács Z., Discacciati M., Samhaber W. (2009). Modeling of amino acid nanofiltration by irreversible thermodynamics, *Journal of Membrane Science*, 332, 38–49, https://doi.org/10.1016/j.memsci.2009.01.034.
79. Al-Zoubi H., Hilal N., Darwish N.A., Mohammad A.W. (2007). Rejection and modelling of sulphate and potassium salts by nanofiltration membranes: neural network and Spiegler–Kedem model, *Desalination*, 206, pp. 42–60, https://doi.org/10.1016/j.desal.2006.02.060.
80. Ballet G. T., Gzara L., Hafiane A., Dhahbi M. (2004). Transport coefficients and cadmium salt rejection in nanofiltration membrane, *Desalination*, 167, pp. 369-376, https://doi.org/10.1016/j.desal.2004.06.148.
81. Mandale S., Jones M. (2010). Membrane transport theory and the interactions between electrolytes and non-electrolytes, *Desalination*, 252, pp. 17–26, https://doi.org/10.1016/j.desal.2009.11.007.

82. Hassan A.R., Ali N., Abdull N., Ismail A.F. (2007). A theoretical approach on membrane characterization: the deduction of fine structural details of asymmetric nanofiltration membranes, *Desalination*, 206, pp. 107–126, https://doi.org/10.1016/j.desal.2006.06.008.
83. Ismail A.F., Hassan A.R. (2004). The deduction of fine structural details of asymmetric nanofiltration membranes using theoretical models, *Journal of Membrane Science*, 231, pp. 25–36, https://doi.org/10.1016/j.memsci.2003.10.024.
84. Dijkstra M.F.J., Bach S., Ebert K. (2006). A transport model for organophilic nanofiltration, *Journal of Membrane Science*, 286, pp. 60–68, https://doi.org/10.1016/j.memsci.2006.09.012.
85. Drews A., Klahm T., Red B, Saygili M., Baumgarten G., Kraume M. (2003). Nanofiltration of CIP waters from iodine X-ray contrast media production: process design and modelling, *Desalination*, 159, pp. 119-129, https://doi.org/10.1016/S0011-9164(03)90064-6.
86. Das C., De S.(2009). Steady state modeling for membrane separation of pretreated liming effluent under cross-flow mode, *Journal of Membrane Science*, 338, pp. 175–181, https://doi.org/10.1016/j.memsci.2009.04.029.
87. Noronha M., Mavrov V., Chmiel H. (2002). Simulation model for optimisation of two-stage membrane filtration plants—minimising the specific costs of power consumption, *Journal of Membrane Science*, 202, pp. 217–232, https://doi.org/10.1016/S0376-7388(01)00791-8.
88. Darvishmanesh S., Buekenhoudt A., Degrève J., Van der Bruggen B. (2009). General model for prediction of solvent permeation through organic and inorganic solvent resistant nanofiltration membranes, *Journal of Membrane Science*, 334, pp. 43–49, https://doi.org/10.1016/j.memsci.2009.02.013.
89. Verliefde A.R.D., Cornelissen E.R., Heijman S.G.J., Verberk J.Q.J.C., Amy G.L., Van der Bruggen B., van Dijk J.C. (2009). Construction and validation of a full-scale model for rejection of organic micropollutants by NF membranes, *Journal of Membrane Science*, 339, pp. 10–20. https://doi.org/10.1016/j.memsci.2009.03.038
90. Mattaraj S., Jarusutthirak C., Jiraratananon R. (2008). A combined osmotic pressure and cake filtration model for crossflow nanofiltration of natural organic matter, *Journal of Membrane Science*, 322, pp. 475–483. https://doi.org/10.1016/j.memsci.2008.05.049.
91. Chaabane T., Taha S., Taleb Ahmed M., Maachi R., Dorange G. (2007). Retention modelling of the bivalent cations in crossflow nanofiltration investigation in the porous models, *Desalination*, 204, pp. 359–367, https://doi.org/10.1016/j.desal.2006.02.040.
92. Mohammad A. W., Takriff M.S. (2003). Predicting flux and rejection of multicomponent salts mixture in nanofiltration membranes, *Desalination*, 157, pp. 105 – 111, https://doi.org/10.1016/S0011-9164(03)00389-8.
93. Szymczyk A., Lanteri Y., Fievet P. (2009). Modelling the transport of asymmetric electrolytes through nanofiltration membranes, *Desalination*, 245, pp. 396–407, https://doi.org/10.1016/j.desal.2009.02.003.
94. Bandini S., Vezzani D. (2003). Nanofiltration modeling: the role of dielectric exclusion in membrane characterization, *Chemical Engineering Science*, 58 pp. 3303 – 3326. https://doi.org/10.1016/S0009-2509(03)00212-4.
95. Bason S., Freger V. (2010). Phenomenological analysis of transport of mono- and divalent ions in nanofiltration, *Journal of Membrane Science*, 360, pp. 389–396, https://doi.org/10.1016/j.memsci.2010.05.037.
96. Mohammad A.W., Hilal N., Al-Zoubi H., Darwish N.A., Ali N. (2007). Modelling the effects of nanofiltration membrane properties on system cost assessment for desalination applications, *Desalination*, 206, pp. 215–225, https://doi.org/10.1016/j.desal.2006.02.068.
97. Yaroshchuk A. (2001). Non-steric mechanisms of nanofiltration: superposition of Donnan and dielectric exclusion, *Separation and Purification Technology*, 22-23, pp.143–158, https://doi.org/10.1016/S1383-5866(00)00159-3.
98. Garcia-Aleman J., Dickson J. M. (2004) Mathematical modeling of nanofiltration membranes with mixed electrolyte solutions, *Journal of Membrane Science*, 235, pp. 1–13, https://doi.org/10.1016/j.memsci.2003.11.023.
99. Braeken L., Bettens B., Boussu K., Van der Meeren P., Cocquyt J., J. Vermant, Van der Bruggen B. (2006) Transport mechanisms of dissolved organic compounds in aqueous solution during nanofiltration, *Journal of Membrane Science*, 279 pp. 311–319, https://doi.org/10.1016/j.memsci.2005.12.024.
100. Hilal N., A1-Zoubi H., Darwish N.A., Mohammad A.W., Abu Arabi M. (2004). A comprehensive review of nanofiltration membranes: Treatment, pretreatment, modelling, and atomic force microscopy, *Desalination*, 170, pp. 281-308, https://doi.org/10.1016/j.desal.2004.01.007.
101. Bowen W. R., Cassey B., Jones P., Oatley D. L. (2004). Modelling the performance of membrane nanofiltration—application to an industrially relevant separation, *Journal of Membrane Science*, 242, pp. 211–220, https://doi.org/10.1016/j.memsci.2004.04.028.
102. Chaabane T., Taha S., Cabon J., Dorange G., Maachi R. (2002). Dynamic modeling of mass transfer through a nanofiltration membrane using calcium salt in drinking water, *Desalination*, 152, pp. 275-280, 2002. https://doi.org/10.1016/S0011-9164(02)01074-3.
103. Chaabane T., Taha S., Taleb Ahmed M., Maachi R., Dorange G. (2007). Coupled model of film theory and the Nernst–Planck equation in nanofiltration, *Desalination*, 206, pp. 424–432, https://doi.org/10.1016/j.desal.2006.03.577.
104. Garba Y., Taha S., Gondrexon N., Cabon J., Dorange G. (2000). Mechanisms involved in cadmium salts transport through a nanofiltration membrane: characterization and distribution, *Journal of Membrane Science*, 168, pp.135–141, https://doi.org/10.1016/S0376-7388(99)00314-2.
105. Gomes S., Cavaco S. A., Quina M. J., Gando-Ferreira L. M. (2010) Nanofiltration process for separating Cr(III) from acid solutions: Experimental and modelling analysis, *Desalination*, 254, pp. 80–89, 2010. https://doi.org/10.1016/j.desal.2009.12.010.

106. Mehiguene K., Taha S., Gondrexon N., Cabon J., Dorange G. (2000). Copper transfer modeling through a nanofiltration membrane in the case of temary aqueous solution, *Desalination*, 127, pp135-143,. https://doi.org/10.1016/S0011-9164(99)00198-8.
107. Palmeri J., Sandeaux J., Sandeaux R., Lefebvre X., David P., Guizard C., Amblard P., Diaz J.-F., Lamaze B. (2002). Modeling of multi-electrolyte transport in charged ceramic and organic nanofilters using the computer simulation program NanoFlux, *Desalination*, 147, pp. 231-236, https://doi.org/10.1016/S0011-9164(02)00541-6.
108. Wesolowska K., Koter S., Bodzek M. (2004). Modelling of nanofiltration in softening water, *Desalination*, 162, pp. 137-151,. https://doi.org/10.1016/S0011-9164(04)00037-2.
109. Cavaco Morao A.I., Szymczyc A., Fievet P., Brites Alves A.M. (2008). Modelling the separation by nanofiltration of a multi-ionic solution relevant to an industrial process, *Journal of Membrane Science*, 322, pp. 320-330, https://doi.org/10.1016/j.memsci.2008.06.003.
110. Wendler B., Goers B., Wozny G. (2002). Nanofiltration of solutions containing surfactants - prediction of flux decline and modelling of mass transfer, *Desalination*, 147, pp. 217–221, https://doi.org/10.1016/S0011-9164(02)00537-4.
111. Noordman T.R., Wesselingh J.A. (2002). Transport of large molecules through membranes with narrow pores The Maxwell–Stefan description combined with hydrodynamic theory, *Journal of Membrane Science*, 210, pp. 227–243, https://doi.org/10.1016/S0376-7388(02)00351-4.
112. Pereira A.M., Rooze J., Timmer M., Kreurentjes J. (2006). An analysis of multi-component mass transfer in solvent nanofiltration, *Desalination*, 199, pp. 37-38, https://doi.org/10.1016/j.desal.2006.03.138.
113. Straatsma J., Bargeman G., van der Horst H.C., Wesselingh J.A. (2002). Can nanofiltration be fully predicted by a model?, *Journal of Membrane Science*, 198, pp. 273–284, https://doi.org/10.1016/S0376-7388(01)00669-X.
114. de Lint W.D.S., Benes N. E. (2004). Predictive charge-regulation transport model for nanofiltration from the theory of irreversible processes, *Journal of Membrane Science*, 243, pp. 365-377, https://doi.org/10.1016/j.memsci.2004.06.041.
115. de Pinto M.N., Semiao V., Geraldes V. (2002). Integrated modeling of transport processes in fluid/nanofiltration membrane systems, *Journal of Membrane Science*, 206, pp. 189–200, https://doi.org/10.1016/S0376-7388(01)00761-X.
116. Geraldes V., Semiao V., de Pinho M. N. (2001). Flow and mass transfer modelling of nanofiltration, *Journal of Membrane Science*, 191, pp. 109–128, https://doi.org/10.1016/S0376-7388(01)00458-6.
117. Geraldes V., Semiao V., de Pinho M. N. (2002). The effect on mass transfer of momentum and concentration boundary layers at the entrance region of a slit with a nanofiltration membrane wall, *Chemical Engineering Science*, 57, pp. 735 – 748, https://doi.org/10.1016/S0009-2509(01)00441-9.
118. Bowen W.R., Jones M.G., Welfoot J.S., Yousef H.N.S. (2000). Predicting salt rejections at nanofiltration membranes using artificial neural networks, *Desalination*, 129, pp. 147-162, https://doi.org/10.1016/S0011-9164(00)00057-6.
119. Yangali-Quintanilla V., Verliefde A., Kim T.-U., Sadmani A., Kennedy M., Amy G. (2009). Artificial neural network models based on QSAR for predicting rejection of neutral organic compounds by polyamide nanofiltration and reverse osmosis membranes, *Journal of Membrane Science*, 342, pp. 251–262, https://doi.org/10.1016/j.memsci.2009.06.048.
120. Kovács Z., Discacciati M., Samhaber W. (2008). Numerical simulation and optimization of multi-step batch membrane processes, *Journal of Membrane Science*, 324, pp. 50–58, https://doi.org/10.1016/j.memsci.2008.06.060.
121. Bader M.S.H. (2006). Nanofiltration for oil-fields water injection operations: analysis of osmotic pressure and scale tendency, *Desalination*, 201, pp.114–120, https://doi.org/10.1016/j.desal.2005.09.041.
122. Elazhar F., Tahaikt M., Achatei A., Elmidaoui F., Taky M., El Hannouni F., Laaziz I., Jariri S., El Amrani M., Elmidaoui A. (2009). Economical evaluation of the fluoride removal by nanofiltration, *Desalination*, 249, pp.154–157, https://doi.org/10.1016/j.desal.2009.06.017.
123. Shaalan H.F., Sorour M.H., Tewflk S.R. (2001). Simulation and optimization of a membrane system for chromium recovery from tanning wastes, *Desalination*, 141, pp. 315-324, https://doi.org/10.1016/S0011-9164(01)85008-6.
124. Iaquinta M., Stoller M., Merli C. (2009). Optimization of a nanofiltration membrane process for tomato industry wastewater effluent treatment, *Desalination*, 245, pp. 314–320, https://doi.org/10.1016/j.desal.2008.05.028.
125. Yaroshchuk A.E. (2000) Optimal charged membranes for the pressure-driven separations of ions of different mobilities: theoretical analysis, *Journal of Membrane Science*, 167, pp. 149–161, https://doi.org/10.1016/S0376-7388(99)00280-X.
126. Bowen W. R., Welfoot J. S. (2002). Predictive modelling of nanofiltration: membrane specification and process optimisation, *Desalination*, 147, pp. 197-203, https://doi.org/10.1016/S0011-9164(02)00534-9.
127. González-Munoz M.J., Parajó J.C. (2010). Diafiltration of Eucalyptus wood autohydrolysis liquors: Mathematical modeling, *Journal of Membrane Science*, 346 pp. 98–104, https://doi.org/10.1016/j.memsci.2009.09.023.
128. Koter S., Koter I. (2006). Theoretical analysis of the performance of composite membrane consisting of the catalytic and nanofiltration layers, *Journal of Membrane Science*, 280, pp. 65–72, https://doi.org/10.1016/j.memsci.2006.01.005.
129. Chilyumova E., Thöming J. (2008). Nanofiltration of bivalent nickel cations — model parameter determination and process simulation, *Desalination*, 224, pp. 12–17, https://doi.org/10.1016/j.desal.2007.04.072.
130. Madaeni S.S., Salehi E. (2009). A new adsorption–transport and porosity combined model for passage of cations through nanofiltration membrane, *Journal of Membrane Science*, 333, pp. 100–109,. https://doi.org/10.1016/j.memsci.2009.02.006.
131. Geens J., Van der Bruggen B., Vandecasteele C. (2006). Transport model for solvent permeation through nanofiltration membranes, *Separation and Purification Technology*, 48, pp. 255–263, https://doi.org/10.1016/j.seppur.2005.07.032.
132. Geens J., Boussu K., Vandecasteele C., Van der Bruggen B. (2006). Modelling of solute transport in non-aqueous nanofiltration, *Journal of Membrane Science*, 281, pp. 139–148, https://doi.org/10.1016/j.memsci.2006.03.028.

133. Lee S., Amy G., Cho J. (2004). Applicability of Sherwood correlations for natural organic matter (NOM) transport in nanofiltration (NF) membranes, *Journal of Membrane Science*, 240 pp. 49–65, https://doi.org/10.1016/j.memsci.2004.04.011.
134. Machado D., Hasson D., Semiat R. (2000). Effect of solvent properties on permeate flow through nanofiltration membranes Part II. Transport model, *Journal of Membrane Science*, 166, pp. 63–69, https://doi.org/10.1016/S0376-7388(99)00251-3.
135. Wang D.-X., Wu L., Liao Z.-D., Wang X.-L., Tomi Y., Ando M., Shintani T. (2006). Modeling the separation performance of nanofiltration membranes for the mixed salts solution with Mg^{2+} and Ca^{2+}, *Journal of Membrane Science*, 284, pp. 384–392, https://doi.org/10.1016/j.memsci.2006.08.004.
136. Morão A., de Amorim M. T. P., Lopes A., Escobar I., Queiroz J. A. (2008). Characterisation of ultrafiltration and nanofiltration membranes from rejections of neutral reference solutes using a model of asymmetric pores, *Journal of Membrane Science*, 319, pp. 64–75, https://doi.org/10.1016/j.memsci.2008.03.019.
137. Yaroshchuk A. (2004). The role of imperfections in the solute transfer in nanofiltration, *Journal of Membrane Science*, 239, pp. 9–15, https://doi.org/10.1016/j.memsci.2004.02.014.
138. Bandini S. (2005). Modelling the mechanism of charge formation in NF membranes: Theory and application, *Journal of Membrane Science*, 264, pp. 75–86, https://doi.org/10.1016/j.memsci.2005.03.055.
139. Shang W.-J., Wang X.-L., Yu Y.-X. (2006). Theoretical calculation on the membrane potential of charged porous membranes in 1-1, 1-2, 2-1 and 2-2 electrolyte solutions, *Journal of Membrane Science*, 285, pp. 362–375, https://doi.org/10.1016/j.memsci.2006.09.005.
140. Katsikaris K., Boukouvalas C., Magoulas K. (2005). Simulation of ultrafiltration process and application to pilot tests, *Desalination*, 171, pp. 1-11, https://doi.org/10.1016/j.desal.2004.02.103.
141. Wang Y., Rodgers V.G.J. (2008). Free-solvent model shows osmotic pressure is the dominant factor in limiting flux during protein ultrafiltration, *Journal of Membrane Science*, 320, pp. 335–343, https://doi.org/10.1016/j.memsci.2008.04.014.
142. Polyakov Y. (2006). Deadend outside-in hollow fiber membrane filter: Mathematical model, *Journal of Membrane Science*, 279, pp. 615–624, 2006. https://doi.org/10.1016/j.memsci.2005.12.056.
143. Cabassud M., Delgrange-Vincentb N., Cabassud C., Durand-Bourlier L., Lainé J.M. (2002). Neural networks: a tool to improve UF plant productivity, *Desalination*, 145 pp. 223-231, https://doi.org/10.1016/S0011-9164(02)00416-2.
144. Yeh H.M., Chen Y.F. (2005). Modified analysis of permeate flux for ultrafiltration in a solid-rod tubular membrane, *Journal of Membrane Science*, 251, pp. 255–261, https://doi.org/10.1016/j.memsci.2004.11.020.
145. Yeh H.M. (2009). Exponential model analysis of permeate flux for ultrafiltration in hollow-fiber modules by momentum balance, *Chemical Engineering Journal*, 147, pp. 202–209, https://doi.org/10.1016/j.memsci.2005.11.002.
146. Munson-McGee S. (2003). An approximate analytical solution for the fluid dynamics of laminar flow in a porous tube, *Journal of Membrane Science*, 197, pp. 223–230, https://doi.org/10.1016/S0376-7388(01)00634-2.
147. Moll R., Moulin Ph., Veyret D., Charbit F. (2002). Numerical simulation of Dean vortices: fluid trajectories, *Journal of Membrane Science*, 197, pp. 157–172, https://doi.org/10.1016/S0376-7388(01)00606-8.
148. Moll R., Veyret D., Charbit F., Moulin P. (2007). Dean vortices applied to membrane process Part II: Numerical approach, *Journal of Membrane Science*, 288, pp. 321–335, 2007. https://doi.org/10.1016/j.memsci.2006.11.037.
149. Taha T., Cui Z.F. (2002). CFD modelling of gas-sparged ultrafiltration in tubular membranes, *Journal of Membrane Science*, 210, pp. 13–27, 2002. https://doi.org/10.1016/S0376-7388(02)00360-5.
150. Dal-Cin M. M., Darcovich K., Bourdoncle M., Khan Z., Caza D. (2006). "Comparison of CFD and one-dimensional Bernoulli solutions of the flow in a plate and frame ultrafiltration module in Z configuration", Journal of Membrane Science, 268, pp. 74–85, https://doi.org/10.1016/j.memsci.2005.05.031.
151. Marcos B., Moresoli C., Skorepova J., Vaughan B. (2009). CFD modeling of a transient hollow fiber ultrafiltration system for protein concentration, *Journal of Membrane Science*, 337, pp. 136–144, https://doi.org/10.1016/j.memsci.2009.03.036.
152. Afonso F, Miramda J.M., Campos J.B.L.M. (2009). Numerical study of BSA ultrafiltration in the limiting flux regime — Effect of variable physical properties, *Desalination*, 249, pp. 1139–1150, https://doi.org/10.1016/j.desal.2009.05.012.
153. Belkacem M., Bahlouli M., Mraoui A., Bensadok K. (2007). Treatment of oil-water emulsion by ultrafiltration: A numerical approach, *Desalination*, 206, pp. 433–439, https://doi.org/10.1016/j.desal.2006.02.069.
154. Schausberger P., Norazman N., Li H., Chen V., Friedl A. (2009). Simulation of protein ultrafiltration using CFD: Comparison of concentration polarisation and fouling effects with filtration and protein adsorption experiments, *Journal of Membrane Science*, 337, 1–8, https://doi.org/10.1016/j.memsci.2009.03.022.
155. Curcio S., Calabrò V., Iorio G. (2009). Reduction and control of flux decline in cross-flow membrane processes modeled by artificial neural networks and hybrid systems, *Desalination*, 236, pp. 234–243, https://doi.org/10.1016/j.desal.2007.10.072.
156. Delgrange-Vincent N., Cabassud C., Cabassud M., Durand-Bourlier L., Laîné J.M. (2000). Neural networks for long term prediction of fouling and backwash efficiency in ultrafiltration for drinking water production, *Desalination*, 131, pp. 353-362, https://doi.org/10.1016/S0011-9164(00)90034-1.
157. Razavi S. M. A., Mousavi S. M., Mortazavi S. A. (2003). Dynamic prediction of milk ultrafiltration performance: A neural network approach, *Chemical Engineering Science*, 58, pp. 4185–4195, https://doi.org/10.1016/S0009-2509(03)00301-4.
158. Razavi M., Mortazavi A., Mousavi M. (2003). Dynamic modelling of milk ultrafiltration by artificial neural network, *Journal of Membrane Science*, 220, pp. 47–58, https://doi.org/10.1016/S0376-7388(03)00211-4.
159. Curcio S., Calabrò V., Iorio G. (2006). Reduction and control of flux decline in cross-flow membrane processes modeled by artificial neural networks, *Journal of Membrane Science*, 286, pp. 125–132, https://doi.org/10.1016/j.memsci.2006.09.024.

160. Cross R. A. (2002). Optimum process designs for ultrafiltration crossflow microfiltration systems, *Desalination*, 145, pp. 159-163, https://doi.org/10.1016/S0011-9164(02)00402-2.
161. Zondervan E., Roffel B. (2008). Modeling and optimization of membrane lifetime in dead-end ultra filtration, *Journal of Membrane Science*, 322, pp. 46–51, https://doi.org/10.1016/j.memsci.2008.05.023.
162. Busca G., Hilal N., Atkin B. P. (2003). Optimisation of washing cycle on ultrafiltration membranes used in treatment of metalworking fluids, *Desalination*, I56, pp. 199-207, https://doi.org/10.1016/S0011-9164(03)00342-4.
163. Childress A. E., Le-Clech P., Daugherty J. L., Chen C., Leslie G. L. (2005). Mechanical analysis of hollow fiber membrane integrity in water reuse applications, *Desalination*, 180, pp. 5-14, https://doi.org/10.1016/j.desal.2004.12.026.
164. Paris J., Guichardon P., Charbit F. ()2002 .Transport phenomena in ultrafiltration: a new two-dimensional model compared with classical models, *Journal of Membrane Science*, 207, pp. 43–58, https://doi.org/10.1016/S0376-7388(01)00752-9.
165. Sarkar D., Bhattacharya A., Bhattacharjee C. (2010). Modeling the performance of a standard single stirred ultrafiltration cell using variable velocity back transport flux, *Desalination*, 261, 89–98, https://doi.org/10.1016/j.desal.2010.05.025.
166. Yeh H.M., Chen Y.F. (2006). Momentum balance analysis of permeate flux for ultrafiltration in tubular membranes with gradually increasing incidental angles of a wired-rod insert, *Journal of Membrane Science*, 278, pp. 205–211, https://doi.org/10.1016/j.memsci.2005.11.002.
167. Lipnizki J., Jonsson G. (2002). Flow dynamics and concentration polarisation in spacer-filled channels, *Desalination*, 146 pp. 213-217, https://doi.org/10.1016/S0011-9164(02)00474-5.
168. Han S.-Ch., Choo K.-H., Choi S.-J., Benjamin M. (2007). Modeling manganese removal in chelating polymer-assisted membrane separation systems for water treatment, *Journal of Membrane Science*, 290, pp. 55–61, https://doi.org/10.1016/j.memsci.2006.12.022.
169. Karasu K., Yoshikawa S., Kentish S., Stevens G. (2009). A model for cross-flow ultrafiltration of dairy whey based on the rheology of the compressible cake, *Journal of Membrane Science*, 341, pp. 252–260, https://doi.org/10.1016/j.memsci.2009.06.018.
170. Chang S., Fane A.G., Waite T.D. (2006). Analysis of constant permeate flow filtration using dead-end hollow fiber membranes, *Journal of Membrane Science*, 268, pp.132–141, https://doi.org/10.1016/j.memsci.2005.06.010.
171. Pak A., Mohammadi T., Hosseinalipour S.M., Allahdini V. (2008). "CFD modeling of porous membranes, *Desalination*, 222, pp. 482-488, https://doi.org/10.1016/j.desal.2007.01.152.
172. Busch J., Cruse A., Marquardt W. (2007). Modeling submerged hollow-fiber membrane filtration for wastewater treatment, *Journal of Membrane Science*, 288 pp. 94–111, https://doi.org/10.1016/j.memsci.2006.11.008.
173. Yoon S.-H., Kim H.-S., Yeom I.-T. (2004). Optimization model of submerged hollow fiber membrane modules, *Journal of Membrane Science*, 234, pp. 147–156, https://doi.org/10.1016/j.memsci.2004.01.018.
174. Tan C. H., Ng H. Y. (2008). Modified models to predict flux behavior in forward osmosis in consideration of external and internal concentration polarizations, *Journal of Membrane Science*, 324, pp. 209–219, https://doi.org/10.1016/j.memsci.2008.07.020.
175. Morehouse J., Lloyd D., Freeman B., Lawler D., Liechti K., Becker E. (2006). Modeling the stretching of microporous membranes, *Journal of Membrane Science*, 283, 430–439, https://doi.org/10.1016/j.memsci.2006.07.024.
176. Kim Y. D., Kim J. Y., Lee H. K., Kim S. C. (2001). A new modeling of asymmetric membrane formation in rapid mass transfer system, *Journal of Membrane Science*, 190, pp. 69–77, https://doi.org/10.1016/S0376-7388(01)00420-3.
177. Kikkinides E.S., Stoitsas K.A., Zaspalis V.T., Burganos V.N. (2004). Simulation of structural and permeation properties of multi-layer ceramic membranes, *Journal of Membrane Science*, 243, pp. 133–141, https://doi.org/10.1016/j.memsci.2004.06.019.
178. Zhang Q., Jing W., Fan Y., Xu N. (2008). An improved Parks equation for prediction of surface charge properties of composite ceramic membranes, *Journal of Membrane Science*, 318, pp. 100–106, https://doi.org/10.1016/j.memsci.2008.02.004.